



Published in final edited form as:

Nature. 2017 August 31; 548(7669): 607–611. doi:10.1038/nature23671.

ISWI chromatin remodellers sense nucleosome modifications to determine substrate preference

Geoffrey P. Dann^{1,†}, Glen P. Liszczak¹, John D. Bagert¹, Manuel M. Müller^{1,†}, Uyen T. T. Nguyen^{1,†}, Felix Wojcik¹, Zachary Z. Brown¹, Jeffrey Bos¹, Tatyana Panchenko^{2,†}, Rasmus Pihl^{1,†}, Samuel B. Pollock^{1,†}, Katharine L. Diehl¹, C. David Allis², and Tom W. Muir¹

¹Department of Chemistry, Princeton University, Frick Laboratory, Princeton, New Jersey 08544, USA

²Laboratory of Chromatin Biology and Epigenetics, The Rockefeller University, New York 10065, USA

Abstract

ATP-dependent chromatin remodellers regulate access to genetic information by controlling nucleosome positions *in vivo*¹. However, the mechanism by which remodellers discriminate between different nucleosome substrates is poorly understood. Many chromatin remodelling proteins possess conserved protein domains that interact with nucleosomal features². Here we used a quantitative high-throughput approach, based on the use of a DNA-barcoded mononucleosome library, to profile the biochemical activity of human ISWI family remodellers in response to a diverse set of nucleosome modifications. We show that accessory (non-ATPase) subunits of ISWI remodellers can distinguish between differentially modified nucleosomes, directing remodelling activity towards specific nucleosome substrates according to their modification state.

Unexpectedly, we show that the nucleosome acidic patch³ is necessary for maximum activity of all ISWI remodellers evaluated. This dependence also extends to CHD and SWI/SNF family remodellers, suggesting that the acidic patch may be generally required for chromatin remodelling.

Reprints and permissions information is available at www.nature.com/reprints.

Correspondence and requests for materials should be addressed to T.W.M. (muir@princeton.edu).

[†]Present addresses: Department of Chemistry, King's College London, 7 Trinity Street, London SE1 1DB, UK (M.M.M.); Bayer Pharma AG, Berlin, Germany (U.T.T.N.); Perlmutter Cancer Center, New York University Langone Medical Center, 430 East 29th Street, Alexandria Center for Life Sciences West Tower, Suite 625, New York, New York 10016, USA (T.P.); Department of Biomedicine, Aarhus University, Aarhus, Denmark (R.P.); University of California, San Francisco, 505 Parnassus Avenue, San Francisco, California 94143, USA (S.B.P.).

Online Content Methods, along with any additional Extended Data display items and Source Data, are available in the online version of the paper; references unique to these sections appear only in the online paper.

Supplementary Information is available in the online version of the paper.

The authors declare no competing financial interests.

Publisher's note: Springer Nature remains neutral with regard to jurisdictional claims in published maps and institutional affiliations.

Author Contributions G.P.D. purified all remodellers, performed all remodelling and nucleosome library experiments, and processed all sequencing data; G.P.D. prepared the nucleosome library with contributions from G.P.L., M.M.M., U.T.T.N., T.P., Z.Z.B., F.W., J.B., R.P. and S.B.P.; G.P.D. and G.P.L. purified RCC1 and Sir3 constructs for nucleosome library binding experiments; G.P.L. performed the qPCR analysis; G.P.D. and K.L.D. synthesized and purified the LANA peptides; J.D.B. performed the PCA analysis; C.D.A. oversaw the preparation of crotonylated histones; G.P.D., J.D.B. and T.W.M. analysed the data; G.P.D., M.M.M. and T.W.M. conceived the project; T.W.M. supervised the study; G.P.D. and T.W.M. wrote the manuscript.

Reviewer Information Nature thanks B. Cairns, F. Pugh and the other anonymous reviewer(s) for their contribution to the peer review of this work.

Critically, remodelling activity can be regulated by modifications neighbouring the acidic patch, signifying that it may act as a tunable interaction hotspot for ATP-dependent chromatin remodellers and, by extension, many other chromatin effectors that engage this region of the nucleosome surface^{4–9}.

Typically, individual members of a chromatin remodelling family possess the same core ATPase subunit (or homologue thereof), but can perform functionally distinct roles within the nucleus². This specialization occurs through partnership with accessory protein subunits, which can offer additional protein binding partners or sensory inputs that direct chromatin remodelling activity to specific genomic loci. The underlying molecular mechanisms that control this functional specialization, however, remain largely unclear. Many ATP-dependent chromatin remodellers possess protein domains that interact with DNA, histones, and histone post-translational modifications (PTMs)², providing the potential for these domains to act as a means to interpret unique chromatin landscapes by modulating binding to nucleosomes or the DNA translocation efficiency of the ATPase. Though these effects have long been proposed, only a small number of studies have described how modifications to nucleosomes, which occur in massive complexity *in vivo*¹⁰, affect remodelling efficacy^{11–17}. To our knowledge, there has been no systematic analysis of how remodelling activity is tuned by the presence of nucleosome modifications.

Recently, we described an approach for accelerated biochemical analysis of chromatin effectors based on the use of DNA-barcoded mononucleosome libraries¹⁸. An expanded version of this library (Fig. 1, Extended Data Figs 1, 2, Supplementary Fig. 2, and Supplementary Table 1) encompassed a broad range of modifications distributed throughout the nucleosome structure and was specifically tailored for studying chromatin remodelling using a modified restriction enzyme accessibility assay¹⁹ (Fig. 2a). We used this library to profile the remodelling behaviour (that is, nucleosome sliding) of seven recombinantly produced human ISWI remodellers; namely the SNF2h ATPase and the ACF, CHRAC, WICH, NoRC, RSF and NURF complexes (Extended Data Fig. 3). In total, this effort generated 784 remodelling rate constants from 28,224 individual kinetic measurements (Fig. 2b, Extended Data Fig. 4, Supplementary Tables 2, 3). Several built-in controls served to validate this dataset. As expected, remodelling activity was, in all cases, negligible in the absence of ATP (Fig. 2c, d, Extended Data Fig. 4, Supplementary Table 3). In addition, and consistent with previous work, nucleosomes containing modifications or mutations in the basic patch of the H4 tail were poor substrates of ISWI remodellers^{15,20}, whereas nucleosomes containing the histone variant H2A.Z led to enhanced remodelling activity¹⁷ (Fig. 2e). Finally, restriction enzyme cleavage of a DNA standard present in the library that is unoccupied by a histone octamer (DNA Standard 2) was always faster than nucleosome remodelling, ensuring its activity was not limiting in our assay.

Inspection of the kinetic data revealed that ISWI remodellers are broadly sensitive to nucleosome modifications, with both stimulatory and inhibitory effects evident for all seven enzymes tested (Fig. 2b and Supplementary Table 3). We performed principal component analysis (PCA) to identify experimental trends that contributed to variability in remodeller activity towards different nucleosome substrates. The first principal component accounted

for the large majority of variance (83%) in the data (Extended Data Fig. 5a). Notably, all remodellers had very similar weight values for PC1, demonstrating that histone modifications that stimulate or impede remodelling tend to do so similarly over all the enzymes tested. This suggests that remodellers share functional motifs (for example, in the common ATPase subunit) that are similarly sensitive to changes in the substrate structure, and/or that certain modifications affect the stability of the nucleosome to make DNA translocation more or less difficult (Supplementary Fig. 3).

The second and third principal components revealed how the activity of the remodellers varies in response to specific nucleosome substrates (Fig. 3a). Notably, PCA showed that the activity of the isolated SNF2h ATPase is distinct from all complexes that incorporate the ATPase for DNA translocation activity, indicating that bound accessory subunits repurpose remodelling activity in response to individual nucleosome modification states. Subsets of the nucleosome library drive differences in remodeller activity; the most prominent of these is the H3K14ac modification, which activates only the NoRC complex (Fig. 3b, Extended Data Fig. 5b, Supplementary Table 4). Indeed, we found many individual cases in which a specific nucleosome type had a broad range of effects across different remodellers (Fig. 3b), providing further evidence that the unique subunit compositions of each complex play a direct role in determining their functional specialization. We also observed that histone modifications located on more accessible regions of the nucleosome (for example, on the flexible tails) showed more variability in their effects across different remodellers than those residing under the DNA, which generally elicited similar behaviour across the remodellers evaluated, probably owing to their ability to alter histone–DNA contacts and affect the DNA translocation efficiency of the ATPase subunit²¹ (Fig. 3c and Extended Data Fig. 6a, b).

Further analysis of the remodelling dataset provided insights into the relationship between remodelling activity and the binding preferences of histone recognition (‘reader’) domains within the ISWI remodellers. This was particularly enlightening for the NoRC, WICH, and NURF complexes, all of which have reader domains within their accessory subunits whose binding preferences have been studied^{22–24}. In the case of the NoRC complex, the binding preferences of associated reader domains were an excellent predictor of remodelling output (Extended Data Fig. 7a). This relationship was much less pronounced for the WICH complex (Extended Data Fig. 7b) and, in the case of the NURF complex, we observed an inverse correlation between expected binding preferences and remodelling activity (Extended Data Figs 7c, 8a). In considering the origins of such behaviour, it is worth noting that binding studies on chromatin factors typically employ isolated reader domains and/or histone-derived peptides^{25,26}. These simplified systems, while often informative, are not subject to the same structural and steric constraints as are present in a more physiological setting. Our data highlight the advantages of performing biochemical measurements with intact chromatin effectors and nucleosomal substrates.

Unexpectedly, we found that a nucleosome in our library in which the so-called ‘acidic patch’³ had been disrupted through mutation was inefficiently remodelled by all ISWI family remodellers examined (Fig. 4a). The nucleosome acidic patch is a unique surface feature created by a cluster of acidic residues within the core regions of histones H2A and H2B that together create a negatively charged cleft on each face of the nucleosome disc (Fig.

4a). This surface epitope has emerged as an important component of chromatin recognition⁴⁻⁹. Through further mutagenesis studies, we showed that ISWI remodelling activity requires a trio of amino acids in H2A (E61, D90 and E92) that are known to form a binding pocket for arginine residues within other *trans*-acting chromatin factors²⁷ (Fig. 4b, Extended Data Fig. 8b). Further implicating this region, remodelling of unmodified nucleosomes by the ACF complex was inhibited by addition of the latency-associated nuclear antigen (LANA) peptide from the Kaposi sarcoma-associated herpes virus, which is known to bind the acidic patch using the arginine anchor paradigm⁸ (Extended Data Fig. 8c). We also found that ATPases from the CHD family (CHD4) and SWI/SNF family (BRG1) of remodellers were sensitive to the acidic patch, suggesting that it may be generally required for chromatin remodelling (Fig. 4b).

The number of proteins known to bind and utilize the acidic patch in their interactions with chromatin is continually rising²⁷. It is thus intriguing to speculate that modifications in the neighbourhood of the acidic patch alter the binding of ligands, perhaps in a differential manner. For example, H2A.Z provides two additional residues that extend the acidic patch and enhance ISWI remodelling activity¹⁷. Other studies hint at this possibility as well²⁸. Analysis of our dataset reveals that ISWI remodelling activity is affected by diverse histone PTMs located near the acidic patch (Fig. 4a). Notably, both stimulation and inhibition of nucleosome sliding activity was observed in response to these PTMs (Fig. 4a, Extended Data Fig. 8d). The activity profile of each remodeller was similar across this substrate set, suggesting that a common sensing mechanism was operational across the ISWI remodeller family. We anticipate that such a mechanism is mediated by the ATPase subunit, as it is the only shared component of the complexes. Consistent with this assignment, the isolated SNF2h ATPase subunit was also found to require an intact acidic patch for activity (Fig. 4a). We imagine that the acidic patch may act by stabilizing a SNF2h–nucleosome interaction, or, in considering known modes of ISWI regulation by nucleosomal epitopes²⁹, we can also envision possible allosteric mechanisms.

On the basis of the above findings, we used our nucleosome library platform to investigate the possibility that certain PTMs or histone variants may act as ‘selectivity filters’ for the acidic patch, granting access to subsets of chromatin effectors. In addition to ISWI remodellers, we observed this to be the case for CHD4, RCC1, and Sir3, all factors that we demonstrate, or have previously been demonstrated^{5,6}, to engage the acidic patch (Fig. 4c, Extended Data Fig. 9, Supplementary Table 3, and Supplementary Table 7). We note that compared to PTMs within histone N-terminal tails, which have been extensively studied with respect to chromatin regulation, those residing within the core of the histone octamer are much more enigmatic²¹. We imagine that the acidic patch is able to act as a compositionally dynamic and regulatable interaction hotspot for chromatin effector proteins (Fig. 4d). By extension, perturbation of this region of the nucleosome through either aberrant PTM installation or mutation could lead to dysregulation of epigenetic processes. Indeed, a mutation in the acidic patch (H2AE56Q) has recently been implicated in human uterine and ovarian carcinomas³⁰.

By performing a systematic analysis of the effects of nucleosome modifications on chromatin remodelling activity, we have generated a dataset that exists as a resource to drive

the design of future biochemical and cell-based studies geared towards further understanding of ISWI regulation. We have also shown that the nucleosome acidic patch is generally required for ISWI remodelling and for the activity of chromatin remodelling enzymes spanning multiple remodelling families. Additionally, our data lead us to propose that the acidic patch is subject to dynamic regulation by nucleosome modifications. Lastly, the library developed herein will have broad utility in chromatin biochemistry, by allowing causal relationships between histone modifications and enzymatic outputs to be explored in an unbiased and quantitative manner.

Methods

Analytical methods

Analytical reversed-phase HPLC (RP-HPLC) was performed on an Agilent 1100 series instrument employing a Vydac C18 column (5 μ m, 4 \times 150 mm) at a flow rate of 1 ml/min. Semi-preparative scale purifications were performed on an Agilent 1100 series instrument employing a Vydac C18 semipreparative column (12 μ m, 10 mm \times 250 mm) at a flow rate of 4 ml/min. Preparative scale purifications were conducted on a Waters DeltaPrep 4000 system equipped with a Waters 486 tunable detector (Waters). A Vydac C18 preparative column (15–20 μ m, 20 \times 250 mm) was used at a flow rate of 20 ml/min. 0.1% TFA in water (HPLC solvent A) and 90% acetonitrile, 0.1% TFA in water (HPLC solvent B) were used as the mobile phases in all RP-HPLC analyses and purifications. Electrospray ionisation mass spectrometry (ESI-MS) analysis was conducted on a MicroTOF-Q II ESI-Qq-TOF mass spectrometer (Bruker Daltonics).

Production and purification of RCC1 and Sir3 constructs

Full-length RCC1 (Uniprot ID: P18754) with an N-terminal 6 \times His-SUMO tag and a C-terminal GST tag and the BAH domain of *Saccharomyces cerevisiae* Sir3⁶ with a C-terminal FLAG-6 \times His tag were subcloned into bacterial expression plasmids (pET, Novagen) for protein production in *Escherichia coli*. In brief, BL21 Rosetta (DE3) cells were transfected with expression plasmids and grown in LB medium at 37 $^{\circ}$ C until they reached an OD₆₀₀ of 0.6. For the 6 \times His-SUMO-RCC1-GST construct, protein expression was induced by the addition of 0.6 mM IPTG overnight at 18 $^{\circ}$ C. For the Sir3-BAH-FLAG-6 \times His construct, protein expression was induced by the addition of 0.6 mM IPTG for 1 h at 37 $^{\circ}$ C. Cells were harvested by centrifugation at 4,000g for 10 min at 4 $^{\circ}$ C, and cell pellets were washed twice with 10 ml of cold PBS per litre of culture. Cells were lysed in 10 ml lysis buffer (40 mM Tris, 1 M NaCl, 5 mM β -mercaptoethanol, 10% glycerol, pH 7.7 at 4 $^{\circ}$ C) per litre of culture by passage through an EmulsiFlex-C3 homogenizer (Avestin). Each protein was initially purified by Ni-NTA affinity chromatography. The 6 \times His-SUMO tag was cleaved from the RCC1 construct by Ulp1 protease, and removed by reverse Ni-NTA affinity chromatography. The RCC1-GST and Sir3-BAH-FLAG-6 \times His constructs were further purified over Superdex 200 10/300 GL and Superdex 75 10/300 GL gel filtration columns (GE Healthcare) equilibrated with gel filtration buffer (50 mM Tris, 100 mM NaCl, 2 mM tris(2-carboxyethyl)phosphine, 10% glycerol), respectively, using an AKTA FPLC system (GE Healthcare) equipped with a P-920 pump and UPC-900 monitor before use in subsequent experiments.

Production and purification of recombinant histones

Unmodified recombinant human histones (H2A, Uniprot ID: Q6FI13; H2B, Uniprot ID: O60814; H3C96A, C110A, Uniprot ID: P68431; H4, Uniprot ID: P62805), histone variants, and histone mutants were produced in and purified from *E. coli*. In brief, BL21 Rosetta (DE3) cells were transfected with histone expression plasmids (pET, Novagen) and grown in LB medium at 37 °C until they reached an OD₆₀₀ of 0.6. Protein expression was induced by the addition of 0.6 mM IPTG for 2–3 h at 37 °C. Cells were harvested by centrifugation at 4,000g for 10 min at 4 °C, and cell pellets were washed twice with 10 ml of cold PBS per litre of culture. Cell pellets were resuspended in 10 ml of cold lysis buffer (50 mM Tris, 100 mM NaCl, 1 mM EDTA, 1 mM 2-mercaptoethanol, pH 7.6 at 4 °C) with cComplete, EDTA-free Protease Inhibitor Cocktail (Sigma-Aldrich) per litre of culture and homogenized by passage several times through an 18-gauge needle. Cells were lysed via sonication and the resulting suspension was centrifuged at 30,000g for 30 min at 4 °C. The inclusion body pellet was washed twice with cold lysis buffer containing 1% Triton-X 100 and once without detergent. Inclusion body pellets were resuspended in 10 ml inclusion body resuspension buffer (6 M guanidine hydrochloride, 20 mM Tris, 1 mM EDTA, 100 mM NaCl, 1 mM DTT, pH 7.5 at 4 °C) per litre of culture, and nutated at 4 °C for 2 h. Resuspensions were then centrifuged at 30,000g for 30 min at 4 °C, and the supernatants were transferred to 3.5 kDa MW cutoff dialysis tubing and dialysed overnight in 2 l low salt urea buffer (7 M urea, 10 mM Tris, 1 mM EDTA, 100 mM NaCl, 1 mM DTT, pH 7.5 at 4 °C). Resuspensions were dialysed for an additional 2 h before loading onto a HiTrap SP HP 5-ml column (GE Healthcare) equilibrated with low salt urea buffer (filtered and degassed). The histones were purified using a gradient over 20 column volumes from low salt urea buffer to high salt urea buffer (7 M urea, 10 mM Tris, 1 mM EDTA, 1 M NaCl, 1 mM DTT, pH 7.5 at 4 °C) on an AKTA FPLC system from GE Healthcare equipped with a P-920 pump and UPC-900 monitor. Histones were further purified using preparative C-18 RP-HPLC. Purified histones were analysed by analytical RP-HPLC and ESI-MS (Supplementary Fig. 2).

Production of modified histones by protein semi-synthesis

H2AK119ub, H2BK120ub, H3K4me3, H3K9ac, H3K9me3, H3K14ac, H3K18ac, H3K18acK23ac, H3K23ac, H3K27ac, H3K27me3, H3KpolyAc, H4K5ac, H4K8ac, H4K12ac, H4K16ac, H4K20ac, and H4KpolyAc histones were prepared by semisynthesis as described previously¹⁸. The semisynthesis of the H3R42me2a histone was conducted as described previously³¹.

Preparation of H2AK5ac, H2AK9ac, H2AK13ac, H2AK15ac, and H2AKpolyAc histones

Proteins were assembled from two pieces: a recombinant fragment was generated encompassing residues 21–129 of histone H2A with an A21C mutation fused to an N-terminal 6×His–SUMO tag. This sequence was inserted into a pET expression plasmid and confirmed by gene sequencing. BL21 Rosetta (DE3) cells were transfected with the plasmid and grown in LB medium at 37 °C until they reached an OD₆₀₀ of 0.6. Protein expression was induced by the addition of 0.6 mM IPTG for 2–3 h. Cells were harvested, lysed, and inclusion bodies were prepared identically as for recombinant histones in this study. The 6×His–SUMO–H2A (21–129)A21C protein was purified by Ni-NTA affinity

chromatography. The sample was dialysed for 2 h in 2 M urea, 50 mM Tris, 200 mM NaCl, 1 mM DTT, pH 7.4 at 4 °C before being moved to an otherwise identical buffer containing 1.5 M urea. Ulp1 protease was added to cleave off the 6×His–SUMO tag and the sample was dialysed overnight at 4 °C. The resulting H2A(21–129)A21C fragment was purified using preparative C-18 RP-HPLC. The final product was characterized by ESI-MS and analytical C-18 RP-HPLC.

H2AK5ac, H2AK9ac, H2AK13ac, H2AK15ac, and H2AKpolyAc peptides corresponding to residues 1–20 with acetylated lysine residues at the indicated positions were synthesized as follows: approximately 500–750 mg Trityl-OH resin (ChemMatrix) was resuspended with 10 ml dichloromethane (DCM) and chlorinated by reaction with 200 µl SOCl₂ on a shaker overnight. The resin was washed thoroughly with DCM and dimethylformamide (DMF) followed by an additional wash with 5% (v/v) *N,N*-diisopropylethylamine (DIEA). 500 mg chlorinated resin was combined with a fourfold excess (relative to resin loading) of hydrazine monohydrate in 2 ml DMF along with an eightfold excess of DIEA. The reaction was stirred on ice for 1 h and subsequently washed with DMF before repeating the reaction with hydrazine/DIEA in DMF to ensure quantitative loading. To ensure all reactive sites on the resin had been consumed, after 1 h, 500 µl methanol was added to the second hydrazine reaction and stirred for an additional 30 min.

The peptides were synthesized on a CEM Discover Microwave Peptide Synthesizer using Fmoc chemistry. Fmoc-acetyllysine was used to incorporate acetyllysine residues at the appropriate positions. For a 0.25 mmol-scale reaction the resin was first swelled in DMF. In between, the resin was washed with DMF and DCM. Each amino acid was dissolved in DMF (200 mM) and introduced to the resin after the deprotection step. DIEA (2 M) in *N*-methylpyrrolidone (NMP) and HOBt (500 mM)/HBTU (500 mM) in DMF were added along with the amino acid to perform each coupling (twice). The resin was then removed from the synthesizer without deprotecting the final Fmoc group for stability in storage. The N terminus of each peptide was manually deprotected with 20% piperidine and acetylated with acetic anhydride. Peptides were cleaved from the resin as C-terminal acyl hydrazides in 95% TFA, 2.5% triisopropylsilane (TIS), and 2.5% water and purified by preparative C-18 RP-HPLC. The final products were characterized by ESI-MS and analytical C-18 RP-HPLC.

Full-length histones were prepared by traceless native chemical ligation of acetylated peptides and the recombinant fragment as previously described¹⁸ and purified by semi-preparative C-18 RP-HPLC. Final products were characterized by analytical C-18 RP-HPLC and ESI-MS (Supplementary Fig. 2).

Preparation of the H2AK118ac histone

A recombinant fragment corresponding to residues 1–112 of H2A was fused to a fused Npu DnaE intein with a C-terminal 6×His tag. This protein was produced in *E. coli* and purified by Ni-NTA affinity chromatography. An α-thioester was installed in the histone fragment by thiolysis (via 2-mercaptoethanesulfonate) of the corresponding intein fusion using a method similar to that previously described³². An H2AK118ac peptide (113–129, A113C) was synthesized as described above (Preparation of H2AK5ac, H2AK9ac, H2AK13ac, H2AK15ac, and H2AKpolyAc histones), with minor modifications. The peptide was

synthesized on Wang resin that was purchased pre-charged with the C-terminal amino acid (Boc-protected lysine). Acetylation of the N-terminal amine with acetic anhydride was omitted after final Fmoc deprotection, and the peptides were cleaved (95% TFA, 2.5% triisopropylsilane (TIS), and 2.5%) as C-terminal carboxylates. The full-length histone was prepared by traceless native chemical ligation of acetylated peptide and the recombinant fragment as previously described¹⁸ and subsequently purified by semi-preparative C-18 RP-HPLC. The final product was characterized by analytical C-18 RP-HPLC and ESI-MS (Supplementary Fig. 2).

Preparation of H2BK5ac, H2BK11ac, H2BK12ac, H2BK15ac, H2BK16ac, and H2BK20ac histones

Proteins were assembled from two pieces: a recombinant fragment was generated encompassing residues 21–125 of histone H2B with an A21C mutation fused to an N-terminal 6× His–SUMO tag. This sequence was inserted into a pET expression plasmid and confirmed by gene sequencing. The recombinant H2B(21–125)A21C fragment was produced and purified using a method analogous to that described for the H2A(21–129)A21C fragment above (Preparation of H2AK5ac, H2AK9ac, H2AK13ac, H2AK15ac, and H2AKpolyAc histones). The final product was characterized by ESI-MS and analytical C-18 RP-HPLC.

H2BK5ac, H2BK11ac, H2BK12ac, H2BK15ac, H2BK16ac, and H2BK20ac peptides corresponding to residues 1–20 with acetylated lysine residues at the indicated positions were synthesized by a method analogous to that described above (Preparation of H2AK5ac, H2AK9ac, H2AK13ac, H2AK15ac, and H2AKpolyAc histones), omitting acetylation of the N-terminal amine with acetic anhydride. Full-length histones were prepared by traceless native chemical ligation of acetylated peptides and the recombinant fragment as previously described¹⁸ and were purified by semi-preparative C-18 RP-HPLC. The final products were characterized by analytical C-18 RP-HPLC and ESI-MS (Supplementary Fig. 2).

Preparation of H2BK108ac, H2BK116ac, H2BK120ac, H2BK125ac histones

H2BK108ac, H2BK116ac, H2BK120ac, and H2BK125ac histones were produced in a similar manner to H2AK118ac as described above (Preparation of the H2AK118ac histone). A recombinant fragment corresponding to residues 1–106 of H2B containing an α -thioester was prepared by thiolysis of fused Npu DnaE intein fusion for ligation to H2BK108ac(107–125, A107C) and H2BK116ac(107–125, A107C) peptides. In addition, a recombinant fragment corresponding to residues 1–116 of H2B containing an α -thioester was prepared by thiolysis of a fused Npu DnaE intein fusion for ligation to H2BK120ac(117–125, A107C) and H2BK125ac(117–125, A117C) peptides. Full-length histones were prepared by traceless native chemical ligation of acetylated peptides and the recombinant fragment as previously described¹⁸ and were subsequently purified by semi-preparative C-18 RP-HPLC. The final products were characterized by analytical C-18 RP-HPLC and ESI-MS (Supplementary Fig. 2).

Preparation of phosphorylated H3 histones

The H3H41ph histone was prepared using a previously described three-piece traceless ligation strategy³¹ with minor modifications. Notably, the middle peptide fragment (residues 29–46, A29C) was synthesized with inclusion of Fmoc-Tyr(PO(OBzl)OH)-OH, which was used to introduce a phosphotyrosine residue at position 41 of H3. The H3S10ph histone was prepared using a two-piece traceless ligation strategy analogous to that described previously for ligation of synthetic peptide fragments corresponding to residues 1–14 of H3 to a recombinant H3 fragment corresponding to residues 15–135 (A15C, C96A, C110A)¹⁸. The N-terminal peptide fragment (residues 1–14) was synthesized with inclusion of Fmoc-Ser(PO(OBzl)OH)-OH to introduce a phosphoserine residue at position 10 of H3. The final products were characterized by analytical C-18 RP-HPLC and ESI-MS (Supplementary Fig. 2).

Preparation of H3K4me1 and H3K4me2 histones

H3K4me1 and H3K4me2 histones were prepared using a two-piece traceless ligation strategy analogous to that described previously for native chemical ligation of synthetic peptide fragments corresponding to residues 1–28 of H3 to a recombinant H3 fragment corresponding to residues 29–135 (A29C, C96A, C110A)¹⁸. The N-terminal peptide fragments (residues 1–28) were synthesized using Fmoc chemistry as previously described using an on-resin alkylation strategy to generate mono and dimethylated lysine residues at position 4 of H3^{33,34}. The final products were characterized by analytical C-18 RP-HPLC and ESI-MS (Supplementary Fig. 2).

Preparation of H3R2 methylated histones

H3R2me and H3R2me2a histones were prepared using a two-piece traceless ligation strategy analogous to that described previously for ligation of synthetic peptide fragments corresponding to residues 1–14 of H3 to a recombinant H3 fragment corresponding to residues 15–135 (A15C, C96A, C110A)¹⁸. The N-terminal peptide fragment (residues 1–14) was synthesized with inclusion of either Fmoc-Arg(Me,Pbf)-OH or Fmoc-ADMA(Pbf)-OH to introduce either a monomethyl or asymmetric dimethyl arginine residue at position 2 of H3. The final products were characterized by analytical C-18 RP-HPLC and ESI-MS (Supplementary Fig. 2).

Preparation of the H3K36me3 histone

The H3K36me3 histone was prepared with a three-piece ligation strategy analogous to that previously described³¹ with minor modifications. Notably, the full-length sequence corresponded to H3 and contained C96A, C110A mutations, and the middle peptide fragment (residues 29–46, A29C) was synthesized with inclusion of Fmoc-Lys(Me₃)-OH, which was used to introduce a trimethyllysine residue at position 36 of H3. The final product was characterized by analytical C-18 RP-HPLC and ESI-MS (Supplementary Fig. 2).

Preparation of H4R3 methylated histones

Synthetic H4 peptides were assembled as alkyl-thioesters (TAMPAL)³⁵ on solid phase. Up to residue 4, amino acids were incorporated using Boc-protected amino acids and *in situ*

neutralization protocols. Side-chain protected amino acids (H4(1–14)R3Me and R3Me2s) were coupled using standard HBTU/DIPEA (2-(1H-benzotriazol-1-yl)-1,1,3,3-tetramethyluronium hexafluorophosphate/diisopropylethylamine) procedures; subsequent couplings were carried out using Fmoc amino acids, thus maintaining acid sensitive sidechain protecting groups (for example, Boc or Pbf). To reduce Fmoc-deprotection cocktail exposure time, the terminal residue could be coupled with Bocprotection. Final Fmoc deprotection was carried out in 1-methylpyrrolidine (25% v/v), hexamethylene imine (2% v/v), HOBt (2% w/v), in NMP-DMSO (1:1); (2) DBU (1% v/v), HOBt (1% w/v) in DMF.

The H4(1–14)R3Me2a thioester peptide was synthesized using resin from above that was split before coupling methyl arginine residues. Following Boc-deprotection, neutralization of the TFA salt (5% (v/v) DIPEA-DMF), and thorough washing with DMF, the resin was washed with 5% (w/v) HOBt-DMF, ensuring the slightly acidic environment necessary to maintain arginine side-chain protonation. Subsequent base-free activation of Fmoc-ADMA, in the presence of peptidyl-resin, was achieved using 5 eq of Fmoc-ADMA-OH, 5 eq of *N,N*-diisopropylcarbodiimide (DIC) and 5.5 eq of HOBt in 10% DMF-DCM, with excess HOBt used to maintain side-chain protonation. Fmoc-deprotection was subsequently mediated using 1-methylpyrrolidine (25% v/v), hexamethylene imine (2% v/v), HOBt (2% w/v), in NMP-DMSO (1:1);³⁶ (2) DBU (1% v/v), HOBt (1% w/v) in DMF, and the described coupling process repeated for subsequent amino acids, with neutralization omitted following Fmoc-deprotection.

Peptides were cleaved from the resin using liquid HF. HF cleavage (10 ml HF/g resin) was performed for 1.5 h at 0–4 °C with 5% (v/v) *p*-cresol as a scavenger. Following HF cleavage, the HF was removed under reduced pressure, peptides were precipitated in ice-cold ether, filtered, dissolved in 40% (v/v) aqueous MeCN containing 0.1% (v/v) TFA, and lyophilized. Peptides were purified by preparative C-18 RP-HPLC and final products were characterized by analytical C-18 RP-HPLC and ESI-MS.

To generate the remaining recombinant portion of H4 suitable for native chemical ligation, the H4(1–14) tail was fused to the hexahistidine-tagged, thrombin cleavable truncated H4 protein bearing an A15C mutation; insertion of the His-tag and thrombin cleavage sequence into the H4 protein between residues 14 and 15 was found to improve expression levels. This approach yielded protein as inclusion bodies, which after Ni²⁺-affinity chromatography was subjected to on-column cleavage with thrombin. By incorporating a mutated thrombin cleavage site (LVPRC), the desired N-terminal cysteine containing H4 fragment could be obtained by extracting the cleaved protein from the column using 8 M urea. The truncated histones were then further purified by preparative C-18 RP-HPLC.

Native chemical ligation was performed in 0.1 M sodium phosphate pH 7.5, 6 M guanidine-HCl, 0.1 M NaCl, 60 mM TCEP, 30 mM 4-mercaptophenylacetic acid (MPAA) at 37 °C. Reactions were performed at approximately 3 mM peptide concentration in siliconized 1.5-mL microcentrifuge tubes. Substantially lower yields were obtained when standard polypropylene tubes were used. Ligation products were purified, desulfurized, and purified

by a method analogous to that previously described¹⁸. Final protein products were characterized by analytical C-18 RP-HPLC and ESI-MS (Supplementary Fig. 2).

Preparation of H4K77ac and H4K79ac histones

H4K77ac and H4K79ac histones were produced by a similar method to that described above (Preparation of the H2AK118ac histone). A recombinant fragment corresponding to residues 1–75 of H4 containing an α -thioester was prepared by thiolysis of a fused Npu DnaE intein fusion for ligation to H4K77ac(76–102, A76C) and H4K79ac(76–102, A76C) peptides. Full-length histones were prepared by traceless native chemical ligation of acetylated peptides and the recombinant fragment analogous to that previously described¹⁸ and were subsequently purified by semi-preparative C-18 RP-HPLC. The final products were characterized by analytical C-18 RP-HPLC and ESI-MS (Supplementary Fig. 2).

Preparation of H2BS112GlcNAc

Fmoc-Ser(β -D-GlcNAc(Ac)₃)-OH was synthesized as previously described (using aglycone Fmoc-Ser(OH)-OBn and glycosyl donor GlcNTroc(Ac)₃-Br)³⁷ for use in solid-phase peptide synthesis. Standard Fmoc solid-phase peptide synthesis was used to access the glycopeptide H2B(107–125, S112GlcNAc, A107C). After successful peptide assembly, the peracetylated glycopeptide was deprotected on resin by hydrazinolysis³⁷, cleaved from the resin, and purified by preparative C18 RP-HPLC. The H2B(1–106) α -thioester was obtained by expression and thiolysis of a recombinant intein fusion fragment of H2B, H2B(1–106)GyrA-His₆ as previously described³². A one-pot ligation–desulfurization procedure³⁸ was used to obtain the final glycosylated H2BS112GlcNAc, histone which was purified by semi-preparative C-18 RP-HPLC. The final product was characterized by analytical C-18 RP-HPLC and ESI-MS (Supplementary Fig. 2).

Production and purification of modified histones by amber suppression

All crotonylated histones were produced using amber suppression in *E. coli* as previously described^{39,40}.

Preparation of H3K4ac, H3K36ac, H3K37ac, H3K56ac, H3K64ac, H3K79ac, H3K115ac, H3K122ac, and H4K91ac histones

H3K4ac, H3K36ac, H3K37ac, H3K56ac, H3K64ac, H3K79ac, H3K115ac, H3K122ac histones were prepared by fusing a fused Npu DnaE intein to the C terminus of H3 (H3C96A, C110A) or H4 and produced using amber suppression in *E. coli* as previously described^{12,41}. Following purification, all proteins were characterized by analytical C-18 RP-HPLC and ESI-MS (Supplementary Fig. 2).

Synthesis of LANA peptides

Two LANA peptides⁸ corresponding to residues 2–22 with a norleucine at position 6 substituted for methionine were prepared. The first contained the otherwise native sequence, and the second had residues 8–10 (LRS) mutated to alanine, which is known to hinder nucleosome binding⁸. Peptides were synthesized on a CEM Discover Microwave Peptide Synthesizer using Fmoc chemistry and a ChemMatrix Rink amide resin (0.47 mmol/g).

Following chain assembly, peptides were cleaved from the resin using 95% TFA, 2.5% TIS, and 2.5% water and purified by C-18 RP-HPLC. Final products were characterized by analytical C-18 RP-HPLC and ESI-MS (Supplementary Fig. 4).

Production of chromatin remodellers in Sf9 cells

All chromatin remodellers used in this study were produced in Sf9 cells using a baculovirus expression vector system. The SNF2h (Uniprot ID: O60264), ACF1 (Uniprot ID: Q9NRL2), WSTF (Uniprot ID: Q9UIG0), CHRAC-15 (Uniprot ID: Q9NRG0), and CHRAC-17 (Uniprot ID: Q9NRF9) coding sequences were a gift from R. Kingston (Harvard University). The RSF1 (Uniprot ID: Q96T23) coding sequence was a gift from D. Reinberg (New York University). The BPTF (Uniprot ID: Q12830, isoform 4) coding sequence was a gift from C. D. Allis (Rockefeller University). The SNFL, TIP5 (Uniprot ID: Q9UIF9, isoform 1), CHD4 (Uniprot ID: Q14839), and RbAp46 (Uniprot ID: Q16576) coding sequences were purchased from Open Biosystems. The SNF2L coding sequence was purchased as an inactive splice variant⁴² with an insertion that was deleted using standard molecular cloning procedures to yield the active variant (Uniprot ID: P28370, isoform 2). pFastBac1-Flag-BRG1 was a gift from R. Kingston (Addgene plasmid # 1957)⁴³. All coding sequences were confirmed by Sanger sequencing. All coding sequences were subcloned into vectors compatible with bacmid generation by standard restriction enzyme cloning methods or Gibson Assembly (NEB) with FLAG affinity tags introduced suitable for purification of all desired proteins and protein complexes (flag denotes N- or C-terminal FLAG affinity tag): pFastBac1-SNF2h-flag, pACEBac1-SNF2h, pACEBac1-ACF1-flag, pACEBac1-WSTF-flag, pACEBac1-CHRAC-15, pACEBac1-CHRAC-17, pACEBac1-TIP5-flag, pACEBac1-flag-RSF1, pFastBac1-flag-BPTF, pACEBac1-RbAp46, pACEBac1-SNF2L, and pACEBac1-CHD4-flag. For bacmid generation, SNF2h, ACF1-flag, WSTF-flag, CHRAC-15, CHRAC-17, TIP5-flag, flag-RSF1, CHD4-flag constructs were transfected into DH10MultiBacTurbo *E. coli* competent cells, and bacmids were produced per manufacturer's instructions (Geneva Biotech). SNF2h-flag, flag-BPTF, SNF2L, RbAp46, and flag-BRG1 constructs were transfected into DH10bac *E. coli* competent cells, and bacmids were produced per manufacturer's instructions (Bac-to-Bac Baculovirus Expression System, ThermoFisher Scientific). To generate virus for protein production, bacmid transfection into Sf9 cells was carried out in 6-well plates. All transfection, viral amplification, and infection steps were performed in a sterile hood. Typically, 1–10 µg of bacmid was transfected into 1×10^6 attached Sf9 cells according to the manufacturer's instructions (Bac-to-Bac Baculovirus Expression System, ThermoFisher Scientific). After transfection, cells were overlaid with 2 ml fresh medium (Sf-900III SFM, Thermo Fisher Scientific) and incubated at 27 °C for 72 h in the dark. The supernatant was collected for virus amplification and cleared by centrifugation to generate the P1 virus. 2% FBS (v/v) was added. Between uses, all viral stocks were stored at 4 °C in the dark. Subsequent steps were carried out in medium with penicillin/streptomycin. To generate the P2 virus, 800 µl P1 virus was added to 20 ml of Sf9 cells in a sterile flask at 2×10^6 cells per ml. Cells were grown at 27 °C in suspension culture in the dark until they reached 40% viability as monitored by trypan blue staining. The culture supernatant was then collected and cleared by centrifugation, and 2% FBS (v/v) was added. To generate the P3 virus (used for protein production), 200 µl P2 virus was added to 50 ml of Sf9 cells in a sterile flask at 2

$\times 10^6$ cells per ml. Cells were grown at 27 °C in suspension culture in the dark until they reached 40% viability as monitored by trypan blue staining. The culture supernatant was then collected and cleared by centrifugation, and 2% FBS (v/v) was added. During virus amplification Sf9 cell density was kept at around 2×10^6 cells per ml, diluting if needed, until growth arrested and viability dropped. Aside from the monomeric SNF2h (SNF2h-flag), CHD4 (CHD4-flag), and BRG1 (flag-BRG1) ATPases, individual viruses were directly combined with Sf9 cell cultures to generate the ACF (ACF1-flag, SNF2h), CHRAC (ACF1-flag, SNF2h, CHRACH-15, CHRAC-17), WICH (WSTF-flag, SNF2h), NoRC (TIP5-flag, SNF2h), RSF (flag-RSF1, SNF2h), and NURF (flag-BPTF, SNF2L, RbAp46) complexes. Production of CHD4 and the ACF, CHRAC, WICH, NoRC, and RSF complexes was carried out by adding a 1:1,000 dilution of each P3 virus to Sf9 suspension cultures at 2×10^6 cells per ml. Cells were harvested by centrifugation after 72 h at 27 °C in the dark. Production of SNF2h, BRG1, and the NURF complex was carried out by adding a 1:100 dilution of P3 virus to Sf9 suspension cultures at 2×10^6 cells per ml. Cells were harvested by centrifugation after 48 h at 27 °C in the dark. All proteins and protein complexes were purified by first washing harvested cell pellets with 10 ml of cold TBS (50 mM Tris, 150 mM NaCl, pH 7.5 at 4 °C) per 50 ml of culture. Washed pellets were resuspended in 400 μ l of cold nuclear extraction buffer A (buffer A; 10 mM HEPES, pH 7.9, 10 mM KCl, 0.1 mM EDTA, 0.1 mM EGTA) with 1 mM DTT, cOmplete, EDTA-free Protease Inhibitor Cocktail (Sigma-Aldrich), and 0.5 mM PMSF per 10 ml of suspension culture and swelled on ice for 15 min. 25 μ l of 10% IGEPAL CA-630 per 400 μ l of buffer A were then added, and the cells were vortexed briefly for lysis. Nuclei were spun down at 4 °C for 30 s at 17,000g and the supernatant was removed. The nuclei were washed once with 400 μ l of cold buffer A (with 1 mM DTT, cOmplete, EDTA-free Protease Inhibitor Cocktail, and 0.5 mM PMSF) per 10 ml of suspension culture. The resulting nuclear pellet was resuspended in 50 μ l of cold nuclear extraction buffer B (buffer B, 20 mM HEPES, pH 7.9, 400 mM KCl, 1 mM EDTA, 1 mM EGTA, 10% glycerol) with 1 mM DTT, cOmplete, EDTA-free Protease Inhibitor Cocktail, and 0.5 mM PMSF per 10 ml of suspension culture. Nuclear pellets were then incubated with end-over-end rotation for 15 min at 4 °C. Nuclear debris was then spun down at 4 °C for 10 min at 17,000g. The supernatant (nuclear extract) was removed for FLAG affinity purification of remodellers. 1.5 μ l (3 μ l of 50% slurry) of anti-FLAG M2 beads (Sigma-Aldrich) per millilitre of suspension culture were used for purification. First, beads were washed twice with 10 bead volumes of BC-100 buffer (20 mM HEPES, 100 mM KCl, 0.2 mM EDTA, 10% glycerol, 1 mM DTT, 0.2 mM PMSF, pH 7.9). The nuclear extract was diluted twofold with BC-0 buffer (BC-100 buffer without KCl) and centrifuged at 4,000g for 10 min at 4 °C. The supernatant was removed from any precipitation, added directly to the washed anti-FLAG M2 beads, and incubated for 1 h at 4 °C with end-over-end rotation. The beads were centrifuged for 5 min at 1,000g and 4 °C, and the supernatant was removed. The beads were washed once with 10 bead volumes of BC-100 buffer, once with 10 bead volumes of BC-300 buffer (BC-100 buffer with 300 mM KCl), and once with 10 bead volumes of BC-100 buffer. Bound protein was eluted by incubation with one bead volume of 0.25 mg/ml FLAG peptide (Sigma-Aldrich) in BC-100 buffer for 20 min at 4 °C. This process was repeated twice. Pure elutions were combined and concentrated using appropriate molecular weight cut-off Vivaspin 500 centrifugal filter units (Vivaproducts) if needed. Concentrations of remodellers were determined using BSA standards and SDS-

PAGE with Coomassie blue staining referencing the intensity of the ATPase subunit for each complex. Following purification, remodellers were aliquoted, flash-frozen in liquid nitrogen and stored at -80°C until use. The purity of ISWI family remodellers (Extended Data Fig. 3a) as well as BRG1 and CHD4 (Supplementary Fig. 5a) was assessed by SDS-PAGE analysis and Coomassie blue staining. Additionally, ATP-dependent nucleosome remodelling activity on unmodified nucleosomes was verified for ISWI family members (Extended Data Fig. 3b) as well as BRG1 and CHD4 (Supplementary Fig. 5b) using a restriction enzyme accessibility assay. All assays were performed in 50 μl reactions with 10 nM unmodified nucleosomes under conditions described below (Nucleosome remodelling rate analysis for validation experiments on single nucleosomes). Time points were taken at 1 min and 60 min, quenched, and deproteinized as described below (Remodelling assays using the nucleosome library). Samples were directly run on a 5% polyacrylamide gel (0.5 \times TBE, 200 V, 40 min). Staining was performed with SYBR Safe DNA gel stain, and gels were imaged on a Typhoon scanner (GE Healthcare). Each remodeller was analysed in the presence and absence of 2 mM ATP. In all cases, the appearance of a lower band at 60 min that is dependent on the presence of ATP (indicative of remodelling) was visible. Concentrations of remodellers used: SNF2h: 200 nM, ACF: 2 nM, CHRAC: 20 nM, WICH: 50 nM, NoRC: 20 nM, RSF: 10 nM, NURF: 50 nM, BRG1: 370 nM, CHD4: 200 nM.

DNA preparation

Barcoded 601 (BC-601) DNA preparation—A PstI restriction site was introduced into a 147-bp 601 sequence via site-directed mutagenesis to detect nucleosome remodelling. The 601 sequence contained 5'-DraIII and 3'-BsaI overhangs and was prepared by digestion of a plasmid containing 16 copies of the desired sequence; full sequence of one repetitive unit (bold, 601 sequence; underline, PstI site):

5'-
GTGACAGGATGTATATATCTGACACGTGCCTGGAGACTAGGGAGTAATC
CCCTTGGCGGTTAAACGCGGGGACAGCGCGTACGTGCGTTAAGC
GGTGCTAGAGCTGTCTACGACCAATTGAGCGGCTGCAGCACCGGGATT
CTCCAG-3'

The plasmid was produced in and purified from DH5 α cells as previously described⁴⁴. Approximately 20 mg of plasmid was obtained from 6 l bacterial culture. Ten milligrams of the plasmid was then digested with BsaI and DraIII (total DNA concentration of 1 mg/ml in the presence of 500 U/ml of each restriction enzyme) at 37 $^{\circ}\text{C}$ overnight. Digested DNA was purified by phenol chloroform extraction and concentrated by ethanol precipitation. The pellet was resuspended in roughly 1 ml of TE buffer (50 mM Tris, 0.1 mM EDTA, pH 7.5) and sucrose was added to a final concentration of 15%. The desired fragment was then purified by polyacrylamide gel electrophoresis (5% polyacrylamide gel, 0.5 \times TBE buffer) using a preparative cell (Bio-Rad). A peristaltic pump in-line with a Foxy R1 fraction collector (Teledyne Isco) was used to collect eluting fractions every 45 s at a flow rate of 1 ml/min. Fractions containing the desired fragment were pooled and concentrated by ethanol precipitation. The pellet was resuspended in water yielding approximately 1–2 mg of 601 DNA. Unique nucleosome identifier barcodes were then individually ligated to 601 DNA fragment using the non-palindromic 5'-DraIII site. Individual oligo pairs were purchased

from Integrated DNA Technologies. Each oligo was dissolved in TE buffer to a concentration of roughly 100 μM . For hybridization, equimolar amounts of oligo pairs (top and bottom strand) were mixed at a concentration of 10 μM each oligo in a volume of 500 μl . Samples were heated on a heat block for 5 min at 95 $^{\circ}\text{C}$, and were subsequently left to cool slowly by placing the heat block on a laboratory benchtop at room temperature for 1 h. Individual oligos contained the following sequence (bold, partial Illumina forward adaptor sequence; underline, unique hexanucleotide nucleosome identifier barcode):

Top strand: 5'-

CTCTTTCCCTACACGACGCTCTTCCGATCTNNNNNN**CACCGC-3'**

Bottom strand: 5'-GTGNNNNNN**NAGATCGGAAGAGCGTCGT**

GTAGGAAAGAGAA-3'

A list of the unique hexanucleotide nucleosome identifier barcodes used in this study can be found in Supplementary Table 5. Relative to the top strand, hybridization resulted in double-stranded BC DNA with a 3' overhang compatible with ligation to the 5'-DraIII overhang on the purified 601 sequence and a 3'-AA dinucleotide overhang to prevent blunt-end ligation of hybridized oligos. In a typical ligation reaction, 0.41 μM of 601 DNA was combined with 1.2 equivalents of double stranded BC DNA and incubated at 37 $^{\circ}\text{C}$ with 0.1 U/ μl T4 polynucleotide kinase (NEB) in a total volume of 100 μl in 1 \times T4 ligase buffer (NEB) for 1 h. Subsequently 5 U/ μl T4 DNA ligase were added, and the mixture was incubated for 1 h at room temperature. Ligation reactions were monitored by native polyacrylamide gel electrophoresis (5% polyacrylamide gel, 0.5 \times TBE, 200 V, 40 min) and staining with SYBR Safe DNA gel stain (ThermoFisher Scientific; Extended Data Fig. 1a). The final product was purified using a Qiagen PCR purification kit and quantified by UV spectroscopy at 260 nm. The final product resulted in a 192-bp DNA fragment composed of the 147-bp 601 sequence and a 45-bp overhang containing a unique hexanucleotide barcode and a partial Illumina forward adaptor sequence (bold, 601 sequence; bold underline, PstI site; underline, unique hexanucleotide nucleosome identifier barcode):

5'-

CTCTTTCCCTACACGACGCTCTTCCGATCTNNNNNN**CACCGCGTGACAGGA
TGTATATATCTGACACGTGCCTGGAGACTAGGGAGTAATCCCCTTGGCG
GTTAAAACGCGGGGACAGCGGTACGTGCGTTTAAGCGGTGCTAGA
GCTGTCTACGACCAATTGAGCGGCTGCAGCACCGGGATTCTCCAG-3'**

The partial Illumina forward adaptor sequence is the 30 bp 5' of the hexanucleotide barcode.

CpG methylated nucleosomal DNA was prepared as described in Extended Data Fig. 1b.

Biotinylated MMTV 'buffer' DNA—Biotinylated mouse mammary tumor virus (MMTV) 'buffer' DNA was prepared by PCR using a MMTV DNA template⁴⁵ with the following primers purchased from Integrated DNA Technologies:

Forward: 5'-biotin-TATCACTTGCAACAGTCCTAACATTACCTC-3' (HPLC purified)

Reverse: 5'-ATCCAAAAACTGTGCCGAGTCGG-3'

The PCR product was purified using a Qiagen PCR purification kit. The final product was quantified by UV spectroscopy at 260 nm and stored at -20 °C.

192-bp DNA fragment used in follow-up studies on individual nucleosomes—

601 DNA used in non-library remodelling assays on individual nucleosomes was generated via PCR. The 147-bp 601 sequence containing a PstI site was inserted into a KS BlueWhite screening vector using standard restriction enzyme techniques. Primers were designed to amplify the 601 sequence with a 45-bp overhang generated from the surrounding vector sequence.

Forward: 5'-GGCCGCTCTAGAACTAGT-3'

Reverse: 5'-CTGGAGAATCCCGGT-3'

DNA fragment generated (bold, 601 sequence; underlined, PstI site):

GGCCGCTCTAGAACTAGTGGATCCGATATCGCTGTTACCGCGTGACAGGA
 TGTATATATCTGACACGTGCCTGGAGACTAGGGAGTAATCCCCTTGGCG
 GTTAAAACGCGGGGGACAGCGCGTACGTGCGTTAAGCGGTGCTAGA
 GCTGTCTACGACCAATTGAGCGGCTGCAGCACCGGGATTCTCC AG

Octamer formation for the nucleosome library

Octamers containing desired histone compositions were assembled as previously described¹⁸ with minor modifications. In brief, histones were dissolved in histone unfolding buffer (6 M guanidine hydrochloride, 20 mM Tris, 5 mM DTT, pH 7.5 at 4 °C) and combined in equimolar ratios (0.75 nmol each of desired version of histones H2A, H2B, H3, and H4). The total histone concentration was adjusted to 1 mg/ml, and the mixtures were placed in Slide-A-Lyzer MINI dialysis devices (3.5 kDa MW cutoff, ThermoFisher Scientific) and dialysed at 4 °C against 3 × 400 ml of octamer refolding buffer (2 M NaCl, 10 mM Tris, 0.5 mM EDTA, 1 mM DTT, pH 7.8 at 4 °C) for at least 4 h for each step, with one dialysis step overnight. The mixtures were then transferred to clean microcentrifuge tubes and spun down at 17,000g for 5 min at 4 °C to remove any precipitate. Supernatants were transferred to fresh microcentrifuge tubes, and 50% (v/v) glycerol was added. Octamer concentrations were measured by UV spectroscopy at 280 nm, and stored at -20 °C until use in nucleosome assembly.

Nucleosome reconstitution for the nucleosome library

Nucleosomes were assembled as previously described¹⁸ with minor modifications. In brief, in a typical nucleosome assembly, a crude histone octamer preparation (50 pmol) was combined with the appropriate BC-601 DNA (25 pmol) and biotinylated MMTV 'buffer' DNA (25 pmol) in 70 µl octamer refolding buffer (2 M NaCl, 10 mM Tris, 0.5 mM EDTA, 1 mM DTT, pH 7.8 at 4 °C). Mixtures were placed in Slide-A-Lyzer MINI dialysis devices (3.5 kDa MW cutoff, ThermoFisher Scientific) and dialysed at 4 °C against 200 ml nucleosome assembly start buffer (10 mM Tris, 1.4 M KCl, 0.1 mM EDTA, 1 mM DTT, pH 7.8 at 4 °C) for 1 h at 4 °C. Subsequently, 330 ml nucleosome assembly end buffer (10 mM Tris, 10 mM KCl, 0.1 mM EDTA, 1 mM DTT, pH 7.8 at 4 °C) was added at a rate of 1

ml/min using a peristaltic pump, followed by two final dialysis steps against nucleosome assembly end buffer (1 h and overnight). The dialysis mixture was transferred to a microcentrifuge tube, and removal of biotinylated MMTV 'buffer' DNA-associated side products was accomplished by affinity depletion using 140 μ l MyOne streptavidin T1 coated Dynabead slurry (ThermoFisher Scientific) for 1 h at room temperature. The unbound material in the supernatant was transferred to a clean microcentrifuge tube, and any precipitate was removed by centrifugation. Final nucleosome preparations were quantified by UV spectroscopy at 260 nm. The quality of individual nucleosomes was assessed by native polyacrylamide gel electrophoresis (5% acrylamide gel, 0.5 \times TBE, 200 V, 40 min), followed by ethidium bromide staining. This resulted in a main band migrating around 500 bp (variable depending on the nucleosome variant; Extended Data Fig. 2a). To form the library, nucleosome preparations were directly combined and concentrated using Vivaspin 500 centrifugal filter units (10 kDa MW cutoff, Vivaproducts). The final nucleosome library was analysed by native gel electrophoresis as previously described (Extended Data Fig. 2b). For storage, 20% (v/v) glycerol was added resulting in a final library concentration of approximately 1.5 μ M. Library aliquots were flash frozen in liquid nitrogen, and stored at -80 $^{\circ}$ C until being thawed before use.

Analysis of nucleosome library integrity by antibody pull-down

We assessed nucleosome library integrity by antibody pull-down against a specific histone mark. The nucleosome library (12 fmol of each member) was combined with a modification-specific antibody (anti-H3K4me3, Abcam: ab8580; 15 μ g/ml final concentration) in 100 μ l antibody binding buffer (20 mM Tris, 50 mM NaCl, 5 mM EDTA, 0.1% TWEEN 20) and incubated at room temperature for 1 h. The volume was then brought to a final volume of 200 μ l with antibody binding buffer. Ten microlitres of Pierce Protein G agarose slurry (previously washed with antibody binding buffer) was then added and the mixture was incubated for an additional hour at room temperature to allow antibody binding to the Protein G beads. The beads were then washed four times with antibody binding buffer and incubated with 100 μ l elution buffer (100 mM Tris, pH 7.5, 10 mM EDTA, 1% SDS, 10 mM, 2-mercaptoethanol, 8 U/ml proteinase K) for 90 min at 50 $^{\circ}$ C. DNA was purified using a Qiagen PCR purification kit, and was subsequently quantified using a Qubit high-sensitivity dsDNA quantification kit. DNA was diluted with water to a final concentration of approximately 2 μ g/ μ l. The sample was PCR amplified according to conditions described below (Addition of multiplex barcodes and Illumina forward and reverse adaptor sequences via PCR). An input sample was prepared by directly mixing an equivalent amount of nucleosome library with elution buffer followed by identical sample processing. Sequencing was performed as described in the section 'Illumina sequencing'. Experimental samples were normalized against the input, and, within the experiment, the indicated variant (Extended Data Fig. 2c).

Nucleosome thermal mobility shift experiments

Nucleosome thermal mobility shift experiments were performed using a method similar to that previously described⁴⁵. Octamers and nucleosomes were prepared in a way similar to that previously described⁴⁴ with minor modifications. Nucleosomes were assembled via salt gradient dialysis on a DNA fragment that was PCR amplified from a pTF vector to generate

a 283-bp fragment containing a centrally positioned MMTV sequence (NucA)⁴⁵ with 64 bp of flanking DNA on each side.

Forward: 5'-ATTTATTATGCATTTAGAATAAATTTTGTGTGCGCCCTTG-3'

Reverse: 5'-CAGTCGAAAGACTGGGCCTTTC-3'

DNA fragment generated (bold, MMTV sequence):

5'-
 ATTTATTATGCATTTAGAATAAATTTTGTGTGCGCCCTTGTCGCTGAGGTACCA
 GATCTGATATCACTT**GCAACAGTCCTAACATTCACCTCTTGTGTGTTTGT**
GTCTGTTTCGCCATCCCGTCTCCGCTCGTCACTTATCCTTCACTTTCCAG
AGGGTCCCCCGCAGACCCGGCGACCCTGGTCGGCCGACTGCGGCA
CAGTTTTTTGGATATCGGATCCCGTCAATCGAGAAGGGCG
 ACACCCCTAATTAGCCCGG GCGAAAGGCCAGTCTTTCGACTG-3'

Approximately 1 pmol of each nucleosome type was incubated in assay buffer (50 mM Tris, 150 mM NaCl, pH 7.5) for 1 h at 37 °C or 47 °C. After incubation, 5 µl of 50% sucrose was added to each sample and the samples were run on a 5% TBE gel in 0.5× TBE buffer for 40 min at 200 V. Nucleosomes were visualized by staining with SYBR Gold Nucleic Acid Gel Stain (ThermoFisher Scientific). Unmodified and H3K14cr nucleosomes are not expected to be as mobile as H3T118H and H4R45A nucleosomes, which contain mutations that affect interactions between histones and DNA.

Experiments using the nucleosome library

Remodelling assays using the nucleosome library—Remodelling assays used a restriction enzyme accessibility (REA)-based strategy and were performed similarly to those previously described¹⁹. In each remodelling reaction, 10 nM of library was used along with varying amounts of remodelling enzyme depending on the baseline activity of each protein preparation. Typically, an amount of remodeler that resulted in approximately 50% of unmodified nucleosomes remodelled in 1 h was used (200 nM SNF2h, 2 nM ACF, 5 nM CHRAC, 10 nM WICH, 5 nM NoRC, 40 nM RSF, 5 nM CHD4 and 50 nM NURF). Fifty microlitre remodelling assays were carried out in REA buffer (12 mM HEPES, pH 7.9, 4 mM Tris, pH 7.5, 60 mM KCl, 10 mM MgCl₂, 10% glycerol, and 0.02% (v/v) IGEPAL CA-630) with or without 2 mM ATP and in the presence of 2 U/µl PstI restriction enzyme (NEB). Reactions were pre-incubated for 10 min at 30 °C before initiation by the addition of nucleosomes. Note that ATP (or an equivalent volume of REA buffer in the case of reactions without ATP) was not added until approximately 2.5 min before initiation. After initiation, remodelling assays were carried out for 1 h at 30 °C. Six microliter samples were taken at 1, 2.5, 5, 15, 30, and 60 min and each was quenched with 9 µl quench buffer (10% glycerol, 70 mM EDTA, pH 8, 20 mM Tris, pH 7.7, 2% SDS, 0.2 mg/ml bromophenol blue). Samples were deproteinized with 30 U/ml proteinase K (NEB) for 1 h at 37 °C. DNA was purified using a Qiagen PCR purification kit, eluting in 50 µl TE buffer (50 mM Tris, 0.1 mM EDTA, pH 7.5). For each enzyme, reactions with and without ATP were performed in triplicate. With six time points taken per reaction, this generated 36 samples per enzyme analysed. Samples were quantified using a Qubit high-sensitivity dsDNA quantification kit. DNA was diluted with water to a final concentration of approximately 2 pg/µl. The sample was then

PCR amplified as per conditions described in the section ‘Addition of multiplex barcodes and Illumina forward and reverse adaptor sequences via PCR’.

Pull-down experiments with the RCC1-GST construct using the nucleosome library—Ten microlitres of Pierce Glutathione Agarose slurry was washed four times with 100 µl binding buffer (20 mM Tris, 50 mM NaCl, 5 mM EDTA 0.1% TWEEN 20, pH 7.5). The beads were resuspended in 100 µl binding buffer after the final wash and 1.5 pmol RCC1-GST was added. Binding to the beads was allowed to occur for 1.5 h at room temperature with end-over-end rotation. After incubation, the beads were washed again four times with 100 µl binding buffer. The beads were resuspended in 100 µl binding buffer after the final wash and combined with the nucleosome library (12 fmol of each member). After incubation with end-over-end rotation for 2 h at 4 °C, the beads were washed again four times with 100 µl binding buffer. The beads were then directly resuspended in 100 µl of DNA elution buffer (100 mM Tris, 10 mM EDTA, 1% SDS, 10 mM β-mercaptoethanol, 200 µg/ml proteinase K) and incubated for 1.5 h at 50 °C. At this point, an input sample for normalization was prepared by taking a small amount of nucleosome library, resuspending it in 100 µl DNA elution buffer, and incubating for 1.5 h at 50 °C. DNA from all samples was purified using a Qiagen PCR purification kit, eluting in 50 µl TE buffer (50 mM Tris, 0.1 mM EDTA, pH 7.5). Samples were quantified using a Qubit high-sensitivity dsDNA quantification kit. DNA was diluted with water to a final concentration of approximately 2 pg/µl. The sample was then PCR amplified as per conditions described in the section ‘Addition of multiplex barcodes and Illumina forward and reverse adaptor sequences via PCR’.

Pull-down experiments with the Sir3-BAH-FLAG-6×His construct using the nucleosome library—Ten microlitres anti-FLAG M2 (Sigma-Aldrich) slurry was washed four times with 100 µl binding buffer (20 mM Tris, 50 mM NaCl, 5 mM EDTA 0.1% TWEEN 20, pH 7.5). The beads were resuspended in 50 µl binding buffer after the final wash and 40 pmol Sir3-BAH-FLAG-6×His was added. Binding to the beads was allowed to occur for 1 h at room temperature with end-over-end rotation. After incubation, the beads were washed again four times with 50 µl binding buffer. The beads were resuspended in 40 µl binding buffer after the final wash and combined with the nucleosome library at a final concentration of 40 nM. After incubation with end-over-end rotation for 1 h at room temperature, the beads were washed again four times with 50 µl binding buffer. The beads were then directly resuspended in 100 µl DNA elution buffer (100 mM Tris, 10 mM EDTA, 1% SDS, 10 mM β-mercaptoethanol, 200 µg/ml proteinase K) and incubated for 1.5 h at 50 °C. At this point an input sample for normalization was prepared by taking a small amount of nucleosome library, resuspending it in 100 µl DNA elution buffer, and incubating for 1.5 h at 50 °C. DNA from all samples was purified using a Qiagen PCR purification kit, eluting in 50 µl TE buffer (50 mM Tris, 0.1 mM EDTA, pH 7.5). Samples were quantified using a Qubit high-sensitivity dsDNA quantification kit. DNA was diluted with water to a final concentration of approximately 2 pg/µl. The sample was then PCR amplified as per conditions described below (Addition of multiplex barcodes and Illumina forward and reverse adaptor sequences via PCR).

Addition of multiplex barcodes and Illumina forward and reverse adaptor sequences via PCR

Approximately 10 pg DNA from each purified experimental sample collected from remodelling assays or binding experiments using the nucleosome library was added to a PCR reaction to be amplified using the following primer pair (XXXXXXX, unique hexanucleotide multiplexing barcode):

Forward primer: 5'-
AATGATACGGCGACCACCGAGATCTACTCTTTCCCTACACGACG-3'

Reverse primer: 5'-
CAAGCAGAAGACGGCATAACGAGATXXXXXXXCTGGAGAATCCCGGTG-3'

A list of the unique hexanucleotide multiplexing barcodes used in this study can be found in Supplementary Table 6. Specific amplification of full-length (un-cut) nucleosomal DNA at each assay time point was carried out using a Phusion High-Fidelity PCR kit from NEB and primers flanking the PstI restriction cut site (1 mM dNTPs, 10 pg DNA, 0.5 μ M each primer, 0.02 U/ μ l polymerase) with the following amplification conditions: step 1: 98 °C for 30 s; step 2: 98 °C for 10 s; step 3: 47 °C for 15 s; step 4: 72 °C for 8 s. Steps 2–4 were repeated for 15 cycles followed by a final extension step at 72 °C for 7 min. To ensure reactions remained in the exponential phase and relative abundances of DNA fragments were maintained, qPCR analysis was performed using 10 pg of a chosen remodelling reaction time point using SYBR Green I Dye for detection on an ABI 7900 quantitative PCR instrument. Identical conditions were used as previously described except a 10-s extension time was used (instead of 8 s) owing to the instrument requirements. A mean C_t value of 13.9 was determined (compare to 15 cycles used for amplification of DNA before Illumina sequencing). The following amplicon was generated that is compatible with Illumina sequencing (bold, 601 sequence; bold underlined, PstI site; NNNNNN, unique hexanucleotide nucleosome identifier barcode; XXXXXXX, unique hexanucleotide multiplexing barcode):

5'-AATGATACGGCGACCACCGAGATCTACTCTTTCCCTACACGACG
CTCTTCCGATCTNNNNNNCAACCGGTGACAGGATGTATATATCTGACACG
TGCTGGAGACTAGGGAGTAATCCCTTGGCGGTTAAACGCGGGGG
ACAGCGGTACGTGCGTTAAGCGGTGCTAGAGCTGTCTACGACCAAT
TGAGCGGCTGCAGCACCGGATTCAGXXXXXXATCTCGTATGCCGT
CTTCTGCTTG-3'

The full Illumina forward adaptor sequence is 5' of the unique hexanucleotide nucleosome identifier barcode (NNNNNN). The full Illumina reverse adaptor sequence is 3' of the unique hexanucleotide multiplexing barcode (XXXXXXX). Samples containing unique multiplexing barcodes could be pooled directly after PCR and purified using a Qiagen PCR purification kit in one pot. After purification, samples were subjected to high-throughput DNA sequencing as described in the methods section 'Illumina sequencing'. In each case, the correct amplicon size (250 bp) was verified by agarose gel electrophoresis and staining with EtBr.

Illumina sequencing

Single-end sequencing of barcoded DNA libraries (starting from the forward adaptor and covering the unique nucleosome identifier barcode) was performed by the Lewis Sigler Institute for Integrative Genomics Sequencing Core Facility at Princeton University on an Illumina HiSeq 2500 with read length of 67 bp. Owing to the substantial sequence homogeneity present in samples generated from remodelling experiments, these libraries were diluted with a PhiX control library to enable sequencing. A custom sequencing primer was used to sequence the index read (5' - CAATTGAGCGGCTGCAGCACCGGGATTCTCCAG-3'). This primer annealed to the 601 sequence and the 8-bp index read covered the unique multiplexing barcode.

Nucleosome remodelling experiments in the presence of LANA peptides

Remodelling experiments in the presence of LANA and LANA mutant (LRS to AAA) peptides and rate calculations were performed as described in the methods section 'Nucleosome remodelling rate analysis for validation experiments on individual nucleosomes using a restriction enzyme accessibility assay'. LANA peptides were pre-incubated with unmodified nucleosomes for 10 min on ice before being used in remodelling assays at a final concentration of 10 μ M peptide.

Nucleosome remodelling rate analysis for validation experiments on individual nucleosomes using a restriction enzyme accessibility assay

All remodelling experiments validating results obtained from the nucleosome library were performed on nucleosomes assembled with the 192-bp fragment described above (192-bp DNA fragment used in follow-up studies on single nucleosomes). Remodelling assays were performed as described in the section 'Remodelling assays using the nucleosome library' with some modifications. Experiments involving the NURF complex were carried out using nucleosomes at 10 nM and NURF at 50 nM. Experiments involving the ACF complex were performed using nucleosomes at 10 nM and ACF at 2 nM. Experiments involving CHD4 were carried out using nucleosomes at 10 nM and CHD4 at 5 nM. Experiments involving BRG1 were carried out using nucleosomes at 10 nM and BRG1 at 200 nM. All reactions were carried out in the presence of 2 mM ATP. Time points were taken, quenched, and deproteinized as described above (Remodelling assays using the nucleosome library). Samples were directly run on a 5% polyacrylamide gel (0.5 \times TBE, 200 V, 40 min). Staining was performed with SYBR Safe DNA gel stain and gels were imaged on a Typhoon scanner (GE Healthcare). Densitometry measurements were performed using Image Studio Lite (LI-COR). Rates were determined using GraphPad Prism by fitting to a single exponential decay equation (see Extended Data Fig. 8a, c, d, Supplementary Fig. 6, and section 'Nucleosome remodelling rate analysis for library experiments').

Nucleosome remodelling assays and rate analysis for validation of acidic patch mutant nucleosomes (H2A E61A, D90A, E92) using an electrophoretic mobility shift nucleosome repositioning assay

Octamers and nucleosomes were prepared using a method similar to that previously described⁴⁴ with minor modifications. Nucleosomes were assembled by salt gradient

dialysis on a 227-bp DNA fragment that was prepared using a method similar to that described above (192-bp DNA fragment used in follow-up studies on individual nucleosomes). In this case, primers were designed to amplify the 601 sequence with an 80-bp overhang generated from the surrounding vector sequence.

Forward: 5'-CACTATAGGGCGAATTGGAG-3'

Reverse – 5'-CTGGAGAATCCCGGT-3'

DNA fragment generated (bold, 601 sequence):

CACTATAGGGCGAATTGGAGCTCCACCGCGGTGGCGGCCGCTCTAGA
 ACTA
 GTGGATCCGATATCGCTGTTACCGCGTGACAGGATGTATATATCTGACAC
GTGCCTGGAGACTAGGGAGTAATCCCCTTGGCGGTTAAACGCGGGG
GACAGCGGTACGTGCGTTTAAGCGGTGCTAGAGCTGTCTACG
ACCAATTGAGCGGCTGCAGACCGGGATTC TCCAG

Fifty-microlitre remodelling assays were carried out in assay buffer (12 mM HEPES, pH 7.9, 4 mM Tris, pH 7.5, 60 mM KCl, 10 mM MgCl₂, 10% glycerol, and 0.02% (v/v) IGEPAL CA-630) with 30 nM ACF complex and 90 nM nucleosomes. Reactions were pre-incubated for 10 min at 30 °C before initiation by the addition of nucleosomes. Note that ATP (final concentration equivalent to 2 mM) was not added until approximately 2.5 min before initiation. After initiation, remodelling assays were carried out for 1 h at 30 °C. Six-microlitre time points were taken at 1, 2.5, 5, 15, 30, and 60 min and each was quenched by addition of 6 µl quench buffer (assay buffer with 800 ng/µl sheared salmon sperm DNA (ThermoFisher Scientific)) and placement on ice. Quenched assay samples were directly run on a 5% TBE gel in 0.5× TBE buffer for 40 min at 200 V. Nucleosomes were visualized by staining with SYBR Gold Nucleic Acid Gel Stain (ThermoFisher Scientific).

Densitometry measurements were performed to quantify the movement of nucleosomes away from their initial position using Image Studio Lite (LI-COR). Rates were determined using GraphPad Prism by fitting to a single exponential decay equation (Extended Data Fig. 8b).

Processing of sequencing data for chromatin remodelling experiments using the nucleosome library

As previously noted, each remodelling experiment (per enzyme) generated 36 samples (triplicate reactions with and without ATP with six time points collected per reaction). Individual remodelling experiments were processed as follows: 67-bp single-end and 8-bp index reads were imported into Galaxy (Princeton University installation). Corresponding read pairs (single-end and index) generated from the same fragment were joined to generate single nucleotide sequences that contained both a unique nucleosome identifier barcode and related unique multiplexing barcode. All reads were then split into separate FASTQ files (36 in total) based on their unique multiplexing barcodes using Galaxy's Barcode Splitter tool. Each FASTQ file was exported from Galaxy, and occurrences of each unique nucleosome identifier barcode within each file were counted using a custom R script. This resulted in individual data points composed of a distinct number of read counts associated with a unique nucleosome identifier barcode and a unique multiplexing barcode.

Also, included in the nucleosome library was a non-nucleosomal DNA fragment identical to BC-601 DNA except that it did not contain a PstI site (DNA Standard 1). It was carried with the sample from the initiation of remodelling experiments through Illumina sequencing, and used as an internal reference to normalize relative abundances of DNA between multiplexed samples. After normalization, sample read counts were organized by time point or experimental condition (with or without ATP) and nucleosome type (Supplementary Table 2). At this point, nucleosomes 71, 78, and 113 were removed from further analysis as their unique nucleosome identifier barcodes created an additional PstI site with the surrounding nucleotide sequence.

Processing of sequencing data for binding experiments using the nucleosome library

Barcode sorting was performed as described in the section ‘Processing of sequencing data for chromatin remodelling experiments using the nucleosome library’. To account for variation in abundance of individual library members, raw read counts (Supplementary Table 7) for each nucleosome were first normalized to corresponding values from the input sample. Note that data from a single input sample was used for processing all pull-down experiments. To better visualize how nucleosome modifications or mutations affect binding, these values were then normalized to one of the unmodified nucleosomes in the nucleosome library (nucleosome 42, see Supplementary Table 1) to calculate relative affinity measurements for all nucleosome library members.

Nucleosome remodelling rate analysis for library experiments

For each enzyme, remodelling rate constants per nucleosome were calculated for experimental triplicates in GraphPad Prism. Also, included in the nucleosome library was a non-nucleosomal DNA fragment identical to BC-601 DNA (DNA Standard 2). Nucleosome remodelling data were fit to a 2-phase exponential decay equation (see below). The first phase (k_{fast}) was fixed as the rate of cutting of DNA Standard 2 in each experiment (fit to 1-phase exponential decay equation). The y -intercept was allowed to vary and the plateau was set to zero. Fitting to this model allowed the second phase (k_{slow}) to be determined as the rate of nucleosome remodelling (this parameter was left unconstrained) (see Supplementary Fig. 6 and below). Additionally, to estimate the minimum rate of remodelling capable of being determined by our analysis methods, we averaged the bottom 1% of rates that had 95% confidence interval non-overlapping with zero and calculated the associated error. Any values below this threshold were set equal to it. This included cases where k_{slow} was extremely slow (the curve very flat) and determined to be slightly negative. The remodelling rates of unmodified nucleosomes in the library were then averaged and the associated error was calculated. $\log_2(\text{fold-change})$ values relative to the unmodified nucleosome rate average and associated errors were then computed for each nucleosome in the library. Singular value decomposition of the nucleosome library data was calculated for PCA with the Python module `matplotlib.mlab` (v. 1.4.3).

Fitting the remodelling kinetic data to a 2-phase decay was necessary to account for the presence of free BC-601 DNA for some members in the library—in particular nucleosomes containing polyacetylated H3 and H4 (Supplementary Fig. 6b). Use of a 1-phase exponential decay led to an overestimation of the rate constants (and a poorer fit) for several library

members, owing to the contribution of the free DNA that is rapidly cut by the PstI restriction enzyme, irrespective of remodelling activity (Supplementary Fig. 6a, c). Fitting the data to the 2-phase exponential led to a better fit for those library members. The first phase accounts for the free DNA, whereas the slower second phase reports on the remodelling rate of the nucleosome. Note, the vast majority of library members had minimal free BC-601 DNA and could be analysed equally well using 1- or 2-phase decays (Supplementary Fig. 6e, f). For consistency, we used the 2-phase decay fit throughout. Contributions of free DNA to rate measurements were generally thought to be dependent not on systematic irreproducibility in the nucleosome assembly procedures used in this study, but typically on the relative affinities of certain modified histone octamers for nucleosomal DNA as observed by gel electrophoresis. For example, polyacetylated nucleosomes tended to show such behaviour (Supplementary Fig. 6b). We therefore propose that the amount of free DNA in a nucleosome preparation must be carefully considered when fitting nucleosome remodelling data generated by a restriction enzyme accessibility assay to a 1-phase exponential decay equation. In the case, where an internal standard to measure the rate of cutting of non-nucleosomal DNA is present (DNA standard 2 in our high-throughput nucleosome remodelling assay), data may be better modelled by a 2-phase exponential decay equation to aid in accounting for the presence of any free DNA. This proves advantageous in situations where large numbers of nucleosomes must be prepared and precious material is limited or if nucleosome assembly reactions prove difficult to optimize.

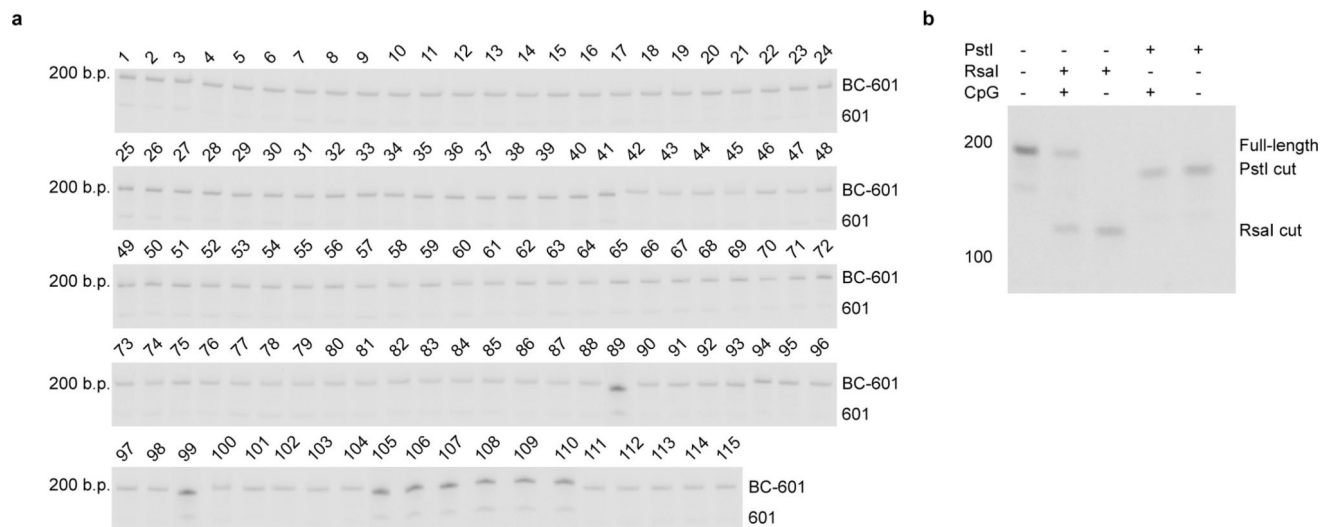
Code availability

A custom R script was used to count individual DNA barcodes in the processing of sequencing data. Requests to access this code may be sent to T.W.M. (muir@princeton.edu).

Data availability

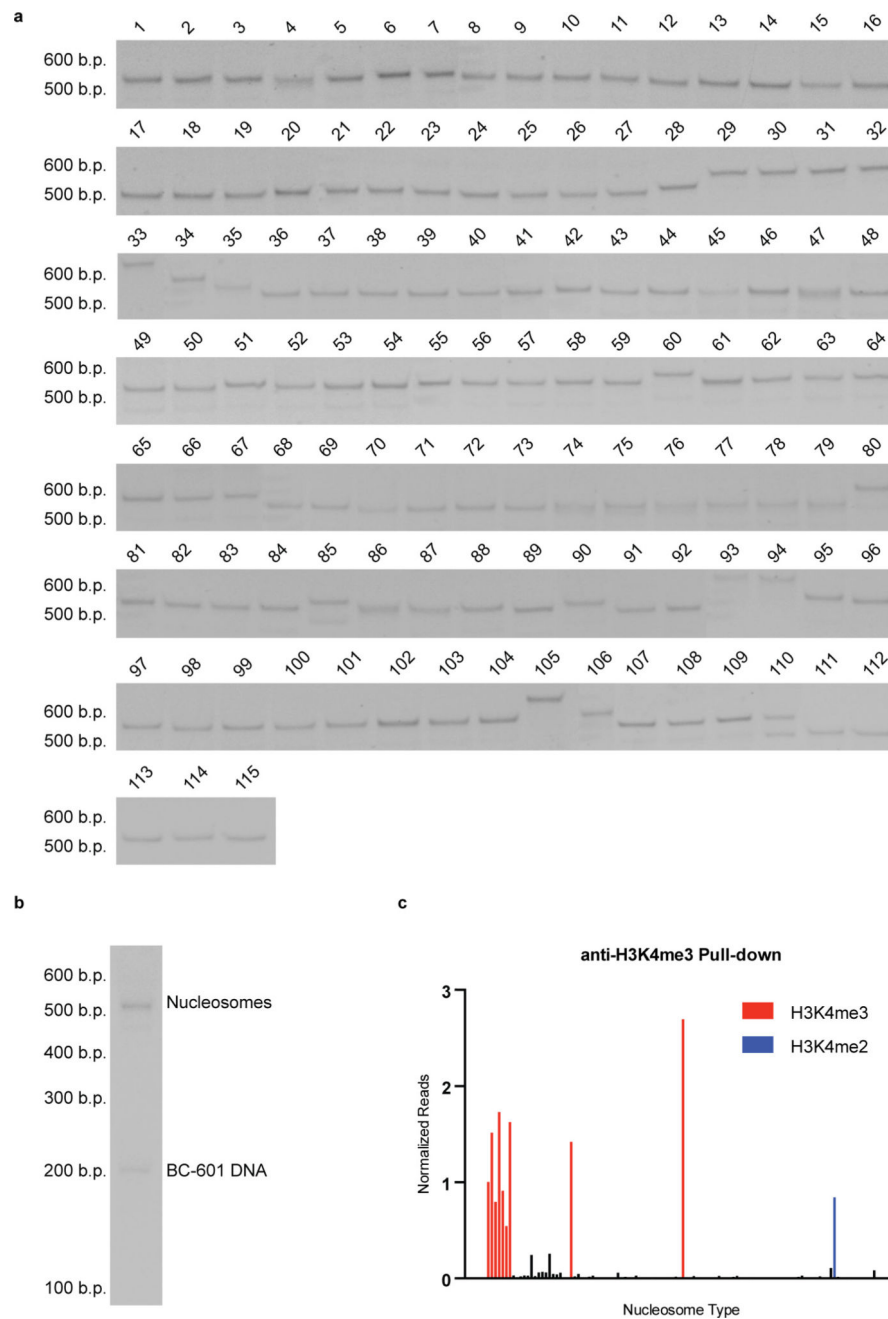
The authors declare that all data supporting the findings of this study are available from the authors and are included within the paper, Extended Data, and its Supplementary Information files.

Extended Data

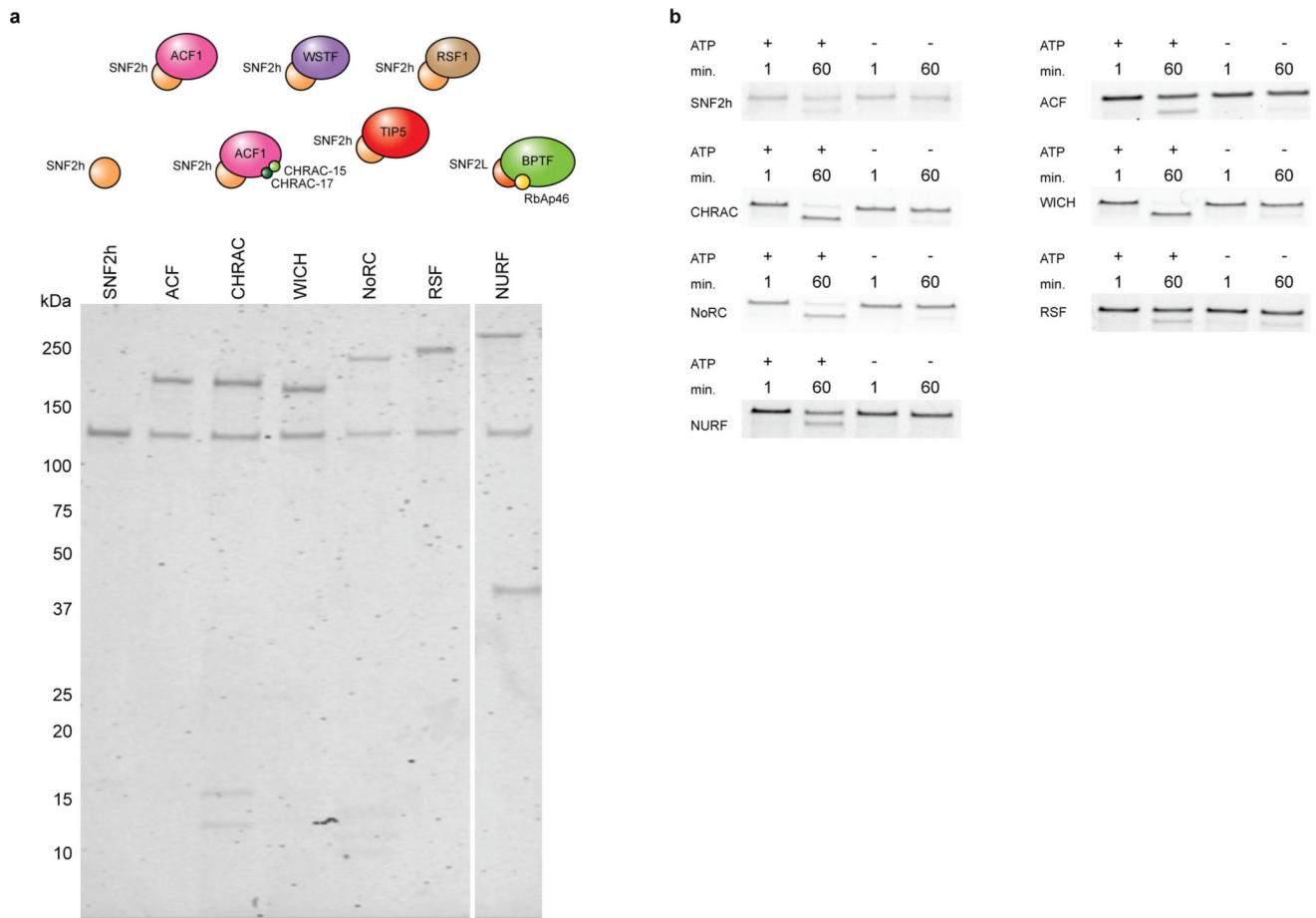


Extended Data Figure 1. Characterization of barcoded 601 (BC-601) DNA

a, BC-601 DNA prepared for all 115 nucleosome library members as described in Methods (Barcoded 601 (BC-601) DNA preparation). Ligation products are 192 bp in size and were visualized by polyacrylamide gel electrophoresis (5% acrylamide, 0.5× TBE, 200 V, 40 min) and staining with SYBR Safe DNA gel stain. A faint band corresponding to unligated 601 DNA (601) is slightly visible in certain cases. **b**, BC-601 DNA for nucleosome 99 (Supplementary Table 1) was CpG methylated by the *M.SssI* methyltransferase (NEB) according to the manufacturer's instructions and characterized by digestion with the *RsaI* restriction enzyme, which is sensitive to CpG methylation, and *PstI*, which is not. For gel source data, see Supplementary Fig. 1.

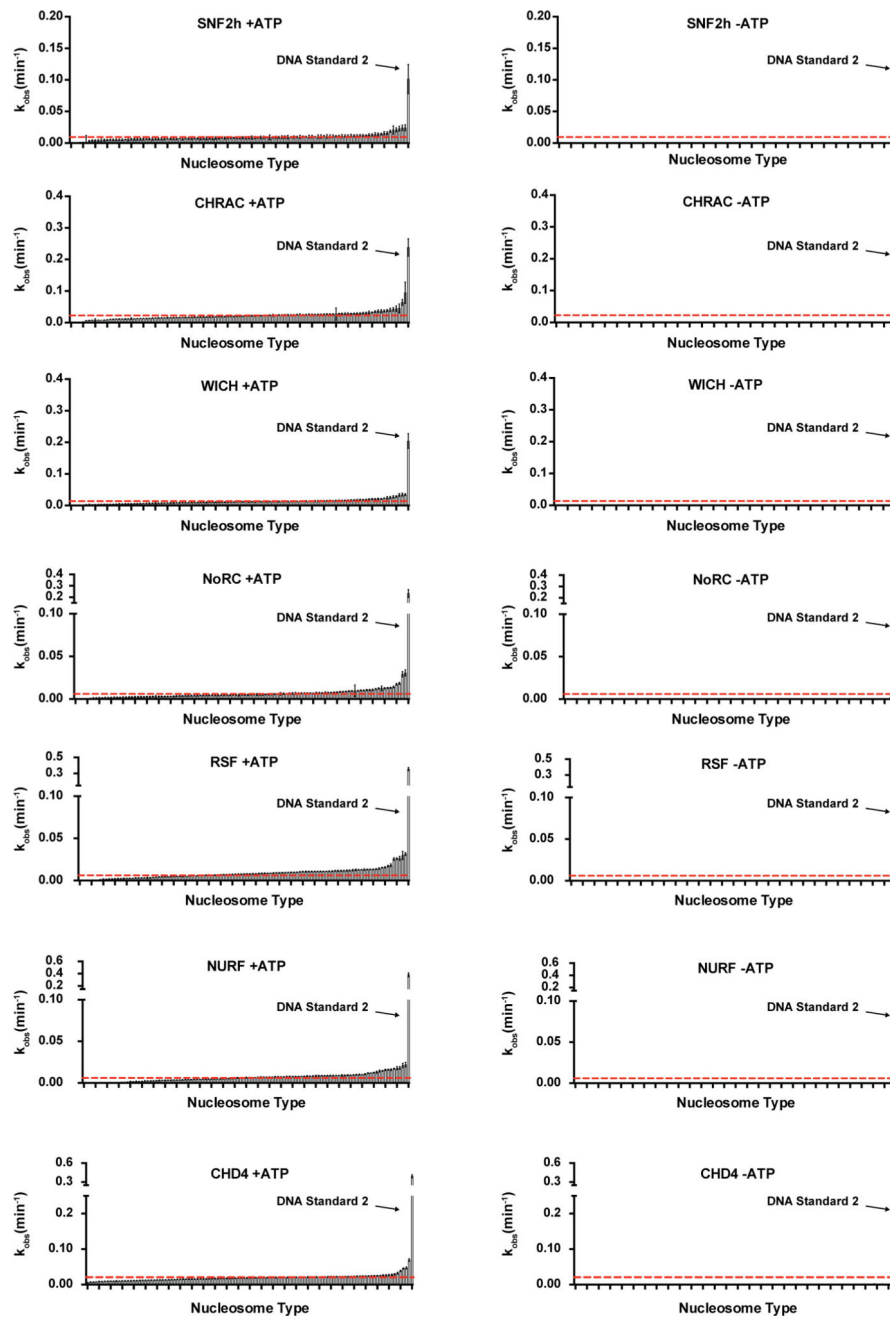


Extended Data Figure 2. Analysis of the quality and integrity of the nucleosome library
a, b, Analysis of individual nucleosome preparations (**a**) and the final library after pooling of nucleosomes (**b**) by native gel electrophoresis and staining with ethidium bromide. **c**, Antibody pull-down of library members using an anti-H3K4me3 antibody. Every nucleosome member containing an H3K4me3 mark (red) was efficiently isolated relative to other library members (black). Notably, the antibody was also able to pull down a nucleosome possessing solely the H3K4me2 mark (blue), indicating a lack of antibody specificity in this case. This experiment was performed once. For gel source data, see Supplementary Fig. 1.

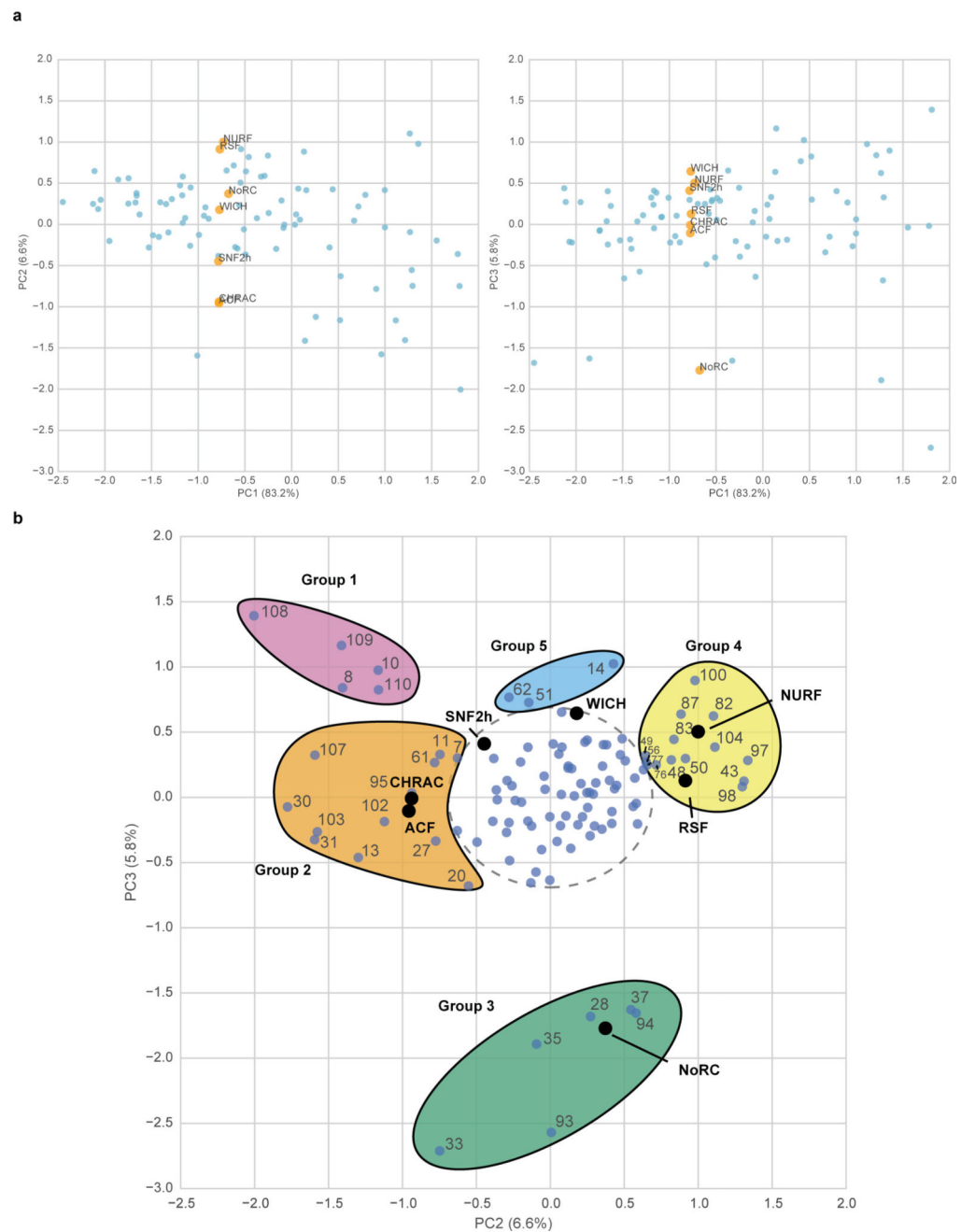


Extended Data Figure 3. Characterization of recombinant ISWI chromatin remodellers

a, Purified chromatin remodellers were run a 4–20% Mini-PROTEAN TGX gel (Bio-Rad) and for 35 min at 180 V. Proteins were stained with Coomassie. The composition of each remodeller–remodelling complex is depicted above each respective lane on the gel. Expected molecular weights: SNF2h: 122 kDa, ACF1: 179 kDa, CHRAC-15: 14.7 kDa, CHRAC-17: 16.9 kDa, WSTF: 171 kDa, TIP5: 208 kDa, RSF1: 164 kDa; migrates at higher apparent molecular weight, SNF2L: 121 kDa, BPTF: 338 kDa, RbAp46: 47.8 kDa. **b**, All remodellers display ATP-dependent nucleosome remodelling activity as detected by a restriction enzyme accessibility assay. For gel source data, see Supplementary Fig. 1.

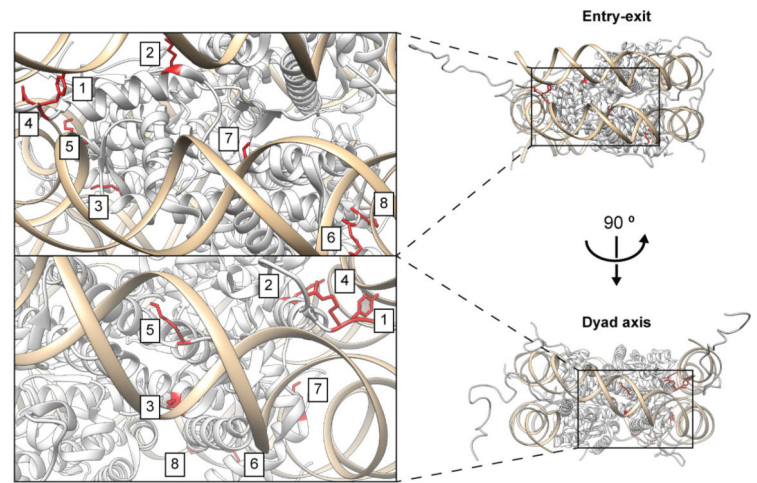
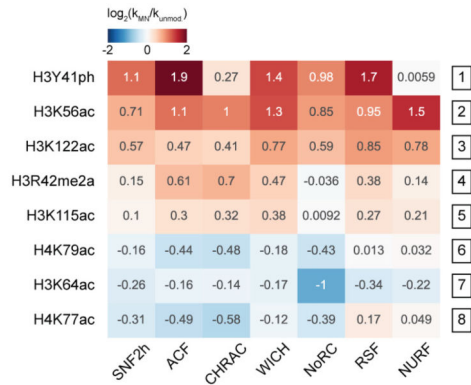


Extended Data Figure 4. Nucleosome remodelling activity is negligible in the absence of ATP
 Bar graphs show individual DNA cleavage rates (k_{MN} , remodelling rates in the case of nucleosomes; see Supplementary Table 3) from library remodelling experiments for each member of the library in the presence of the indicated chromatin remodeller with and without ATP. Rate values were rank ordered and are displayed from low to high. The dashed red line represents the rate of remodelling of unmodified nucleosomes. The related graphs for the ACF complex can be found in Fig. 2d. Data are represented as the mean of experimental replicates \pm s.e.m. ($n = 3$).

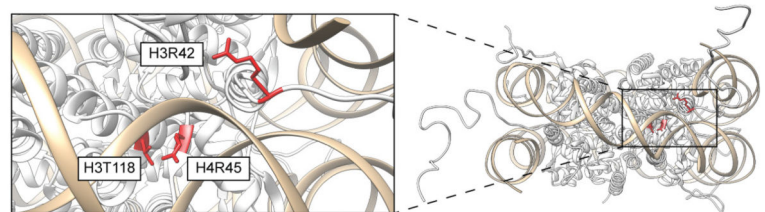
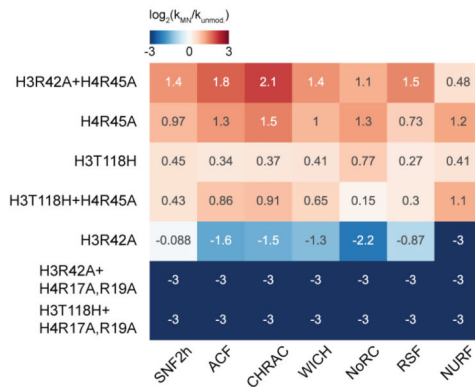


Extended Data Figure 5. Principal component (PC) analysis of library remodelling data
 Percentages show the fractions of the variance accounted for by each PC. Individual nucleosomes are shown in light blue, and PC weight values for each remodeller are shown in either orange or black. Weights are scaled by a factor of 2 for visibility. **a**, PC1 vs. PC2 and PC1 vs. PC3 are plotted. **b**, PC2 vs. PC3 are plotted as in Fig. 3a. Nucleosomes driving differences in remodeller activity were numbered as in Supplementary Table 1 and grouped by their location in PC space (Supplementary Table 4).

a

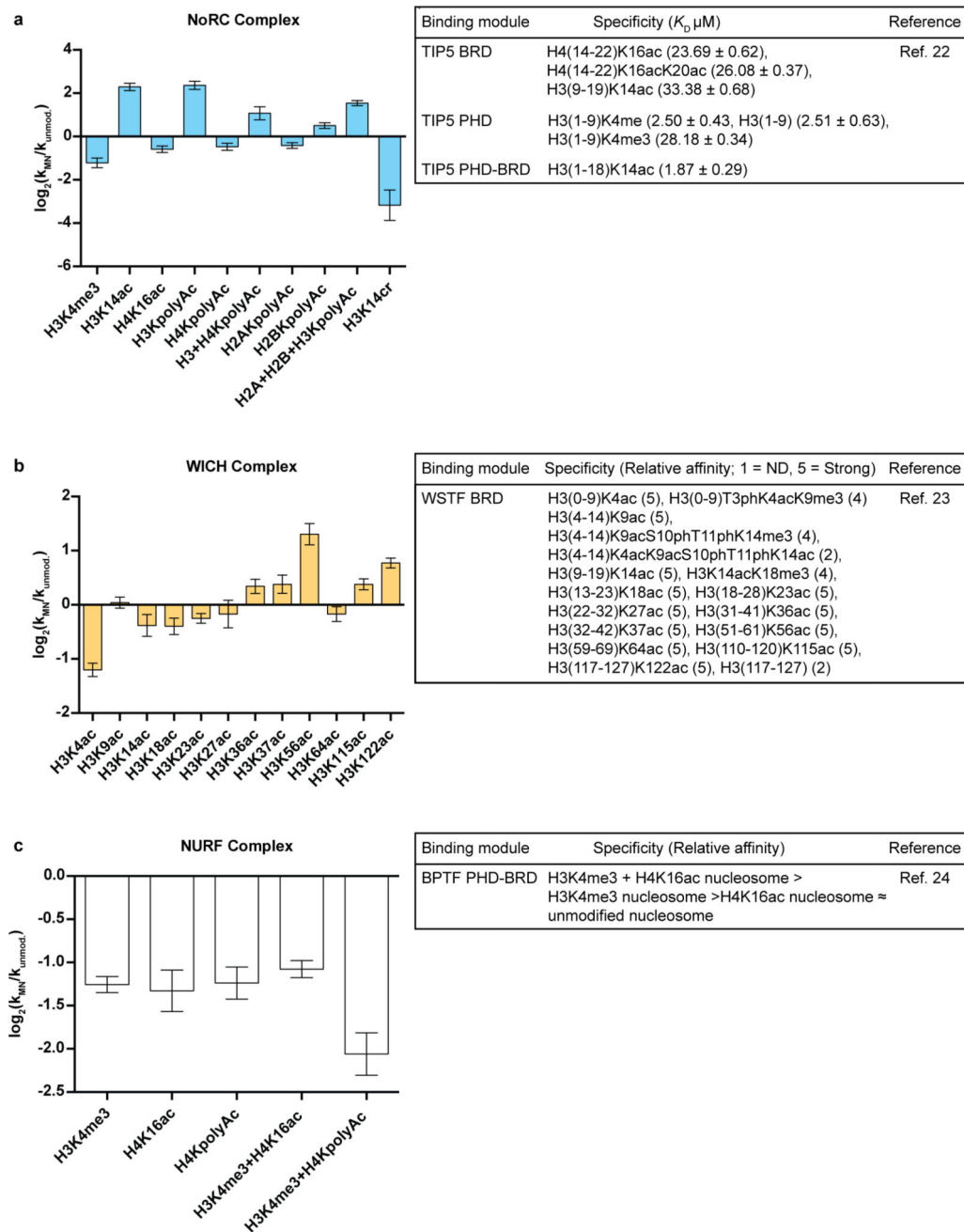


b



Extended Data Figure 6. Alteration of histone–DNA contacts affects remodelling activity

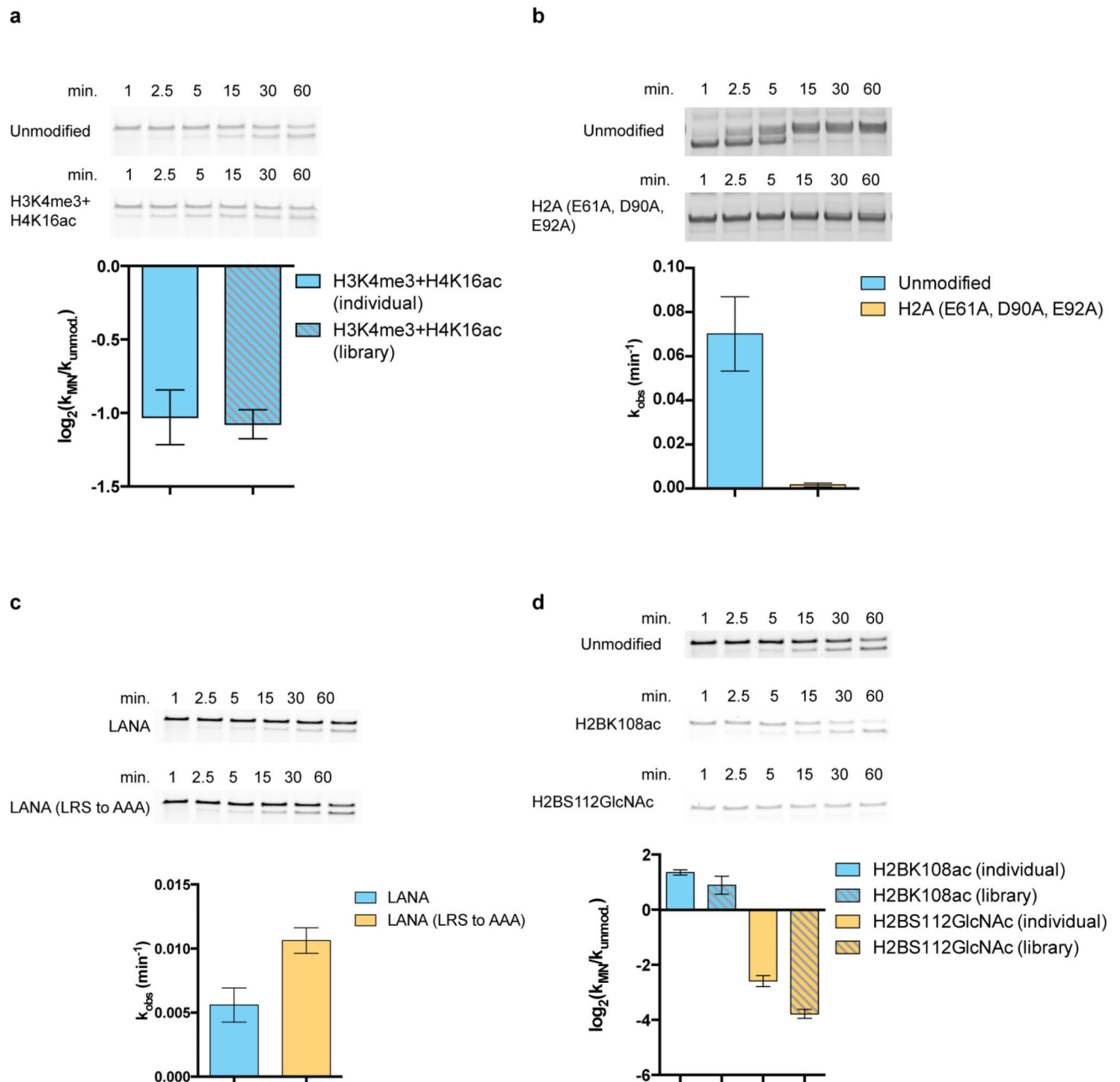
a, Modified histone residues in the nucleosome library that lie under the DNA (tan) are highlighted on the nucleosome (PDB: 1KX5) in red. PTMs are numbered and labelled on the nucleosome structure. Values were capped at -2 and 2 for display purposes. **b**, Histone mutants present in the nucleosome library that lie under the DNA (tan) are highlighted on the nucleosome (PDB: 1KX5) in red. The heatmap is displayed as in **a**. Locations of each mutation are individually labelled on the nucleosome structure. Values were capped at -3 and 3 for display purposes. All histones are unmodified unless otherwise specified.



Extended Data Figure 7. Remodelling of nucleosomes containing modifications preferred by histone recognition domains

Library remodelling data generated by the NoRC (a), WICH (b), and NURF (c) complexes for nucleosomes containing residues known to interact with histone binding modules in accessory subunits of each complex (NoRC: TIP5; WICH: WSTF; NURF: BPTF). Literature binding specificities are displayed in corresponding tables on the right. Bar graphs display \log_2 values of the rate of remodelling of individual nucleosome library members (k_{MN}) relative to unmodified nucleosomes (k_{unmod}). Data are represented as the ratio of the mean of experimental replicates \pm s.e.m. ($n = 3$). Note that H3KpolyAc includes the H3K14ac modification (Supplementary Table 1). All histones are unmodified unless

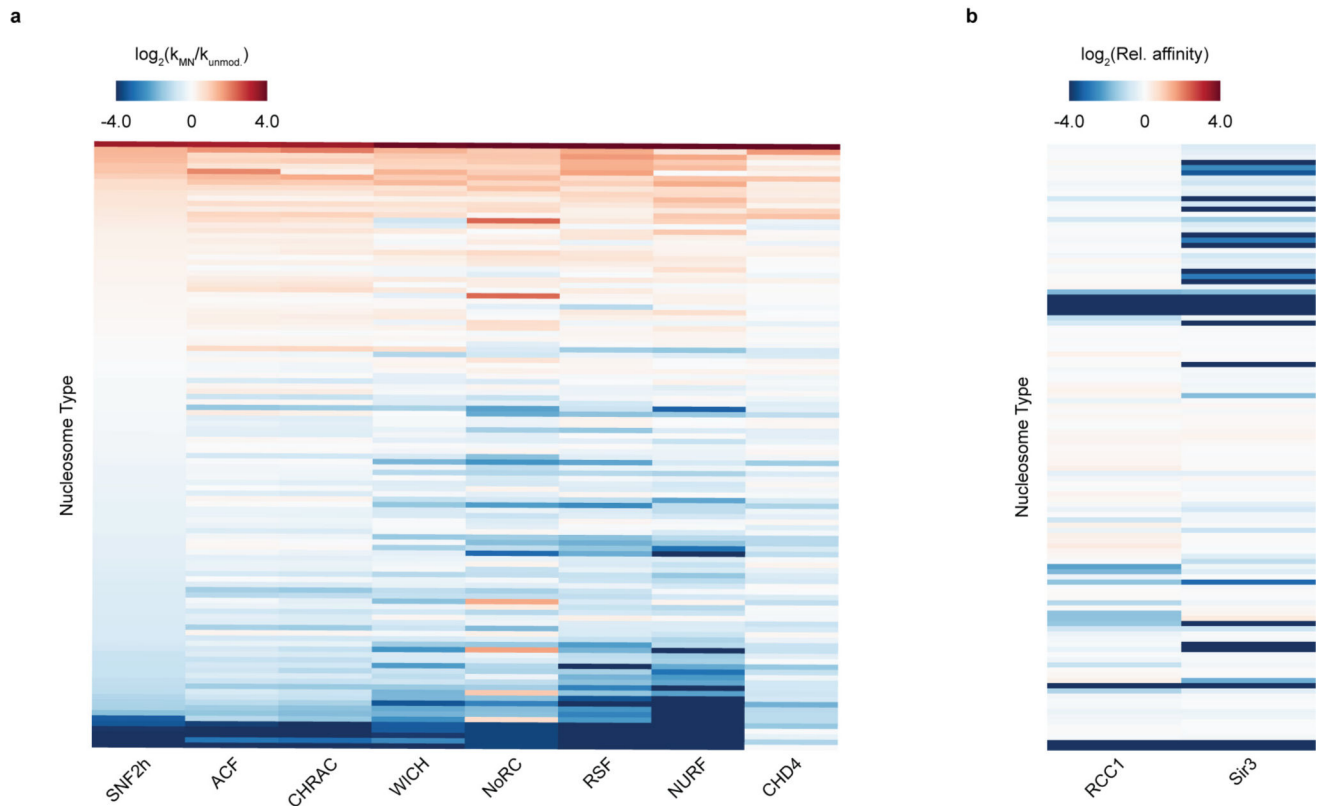
otherwise specified. BRD, bromodomain; PHD, PHD-finger; PHD–BRD, tandem PHD-finger–bromodomain module; ND, not determined.



Extended Data Figure 8. Remodelling assays carried out on individual nucleosomes measured via standard gel-based read-out to validate library data

a, Activity of the NURF complex towards H3K4me3+H4K16ac relative to unmodified nucleosomes as measured in the context of the nucleosome library (library) or individual assays (individual). **b**, Activity of the ACF complex on unmodified and acidic patch mutant nucleosomes. **c**, Remodelling of unmodified nucleosomes is inhibited by the presence of the LANA peptide when compared to a LANA peptide with key binding residues mutated (LRS

to AAA). **d**, Activity of the ACF complex towards nucleosomes modified near the acidic patch (H2BK108ac and H2BS112GlcNac) relative to unmodified nucleosomes as measured in the context of the nucleosome library (library) or individual assays (individual). Gel images of example replicates used to generate densitometry measurements in each subpanel are shown above respective graphs. **a**, **c**, and **d** use a restriction enzyme accessibility assay. **b** uses a nucleosome repositioning electrophoretic mobility shift assay. All histones are unmodified unless otherwise specified. All data are represented as the mean of experimental replicates \pm s.e.m. ($n = 3$). For gel source data, see Supplementary Fig. 1.



Extended Data Figure 9. High-throughput chromatin remodelling and binding data

a, Heat-map displaying ISWI remodelling data (as in Fig. 2b) against the nucleosome library with CHD4 data for comparison. Rows were sorted on the basis of values for SNF2h (low to high). **b**, Heat map displaying binding of chromatin factors RCC1 and Sir3 against the nucleosome library relative to unmodified nucleosomes. Values were capped at -4 and 4 for display purposes. All data are represented as the mean of experimental replicates ($n = 3$).

Supplementary Material

Refer to Web version on PubMed Central for supplementary material.

Acknowledgments

We thank current and former members of the Muir laboratory for discussions and comments; W. Wang and J. Wiggins from the Princeton Sequencing Core Facility; C. Hannon and S. Blythe for writing a custom R script for managing sequencing data; and L. Guerra and L. Beh for advice with data analysis. The SNF2h, ACF1, WSTF,

CHRAC-15, and CHRAC-17 coding sequences were a gift from R. Kingston; the RSF1 coding sequence was a gift from D. Reinberg; the BPTF coding sequence was a gift from C. D. Allis; F.W. was funded by a postdoctoral fellowship from the German Research Foundation (DFG); T.P. was funded by a postdoctoral fellowship from the US National Institutes of Health (GM112365); and this research was supported by the US National Institutes of Health grants P01 CA196539, R37 GM086868 and R01 GM107047.

References

1. Jiang C, Pugh BF. Nucleosome positioning and gene regulation: advances through genomics. *Nat. Rev. Genet.* 2009; 10:161–172. [PubMed: 19204718]
2. Clapier CR, Cairns BR. The biology of chromatin remodeling complexes. *Annu. Rev. Biochem.* 2009; 78:273–304. [PubMed: 19355820]
3. Luger K, Mäder AW, Richmond RK, Sargent DF, Richmond TJ. Crystal structure of the nucleosome core particle at 2.8 Å resolution. *Nature.* 1997; 389:251–260. [PubMed: 9305837]
4. Morgan MT, et al. Structural basis for histone H2B deubiquitination by the SAGA DUB module. *Science.* 2016; 351:725–728. [PubMed: 26912860]
5. Makde RD, England JR, Yennawar HP, Tan S. Structure of RCC1 chromatin factor bound to the nucleosome core particle. *Nature.* 2010; 467:562–566. [PubMed: 20739938]
6. Armache KJ, Garlick JD, Canzio D, Narlikar GJ, Kingston RE. Structural basis of silencing: Sir3 BAH domain in complex with a nucleosome at 3.0 Å resolution. *Science.* 2011; 334:977–982. [PubMed: 22096199]
7. McGinty RK, Henrici RC, Tan S. Crystal structure of the PRC1 ubiquitylation module bound to the nucleosome. *Nature.* 2014; 514:591–596. [PubMed: 25355358]
8. Barbera AJ, et al. The nucleosomal surface as a docking station for Kaposi's sarcoma herpesvirus LANA. *Science.* 2006; 311:856–861. [PubMed: 16469929]
9. Kato H, et al. A conserved mechanism for centromeric nucleosome recognition by centromere protein CENP-C. *Science.* 2013; 340:1110–1113. [PubMed: 23723239]
10. Tan M, et al. Identification of 67 histone marks and histone lysine crotonylation as a new type of histone modification. *Cell.* 2011; 146:1016–1028. [PubMed: 21925322]
11. Ferreira H, Flaus A, Owen-Hughes T. Histone modifications influence the action of Snf2 family remodelling enzymes by different mechanisms. *J. Mol. Biol.* 2007; 374:563–579. [PubMed: 17949749]
12. Neumann H, et al. A method for genetically installing site-specific acetylation in recombinant histones defines the effects of H3 K56 acetylation. *Mol. Cell.* 2009; 36:153–163. [PubMed: 19818718]
13. North JA, et al. Phosphorylation of histone H3(T118) alters nucleosome dynamics and remodeling. *Nucleic Acids Res.* 2011; 39:6465–6474. [PubMed: 21576235]
14. Chatterjee N, et al. Histone H3 tail acetylation modulates ATP-dependent remodeling through multiple mechanisms. *Nucleic Acids Res.* 2011; 39:8378–8391. [PubMed: 21749977]
15. Shogren-Knaak M, et al. Histone H4-K16 acetylation controls chromatin structure and protein interactions. *Science.* 2006; 311:844–847. [PubMed: 16469925]
16. Chatterjee N, et al. Histone acetylation near the nucleosome dyad axis enhances nucleosome disassembly by RSC and SWI/SNF. *Mol. Cell. Biol.* 2015; 35:4083–4092. [PubMed: 26416878]
17. Goldman JA, Garlick JD, Kingston RE. Chromatin remodeling by imitation switch (ISWI) class ATP-dependent remodelers is stimulated by histone variant H2A.Z. *J. Biol. Chem.* 2010; 285:4645–4651. [PubMed: 19940112]
18. Nguyen UT, et al. Accelerated chromatin biochemistry using DNA-barcoded nucleosome libraries. *Nat. Methods.* 2014; 11:834–840. [PubMed: 24997861]
19. He X, Fan HY, Narlikar GJ, Kingston RE. Human ACF1 alters the remodeling strategy of SNF2h. *J. Biol. Chem.* 2006; 281:28636–28647. [PubMed: 16877760]
20. Clapier CR, Nightingale KP, Becker PB. A critical epitope for substrate recognition by the nucleosome remodeling ATPase ISWI. *Nucleic Acids Res.* 2002; 30:649–655. [PubMed: 11809876]

21. Tropberger P, Schneider R. Scratching the (lateral) surface of chromatin regulation by histone modifications. *Nat. Struct. Mol. Biol.* 2013; 20:657–661. [PubMed: 23739170]
22. Tallant C, et al. Molecular basis of histone tail recognition by human TIP5 PHD finger and bromodomain of the chromatin remodeling complex NoRC. *Structure.* 2015; 23:80–92. [PubMed: 25533489]
23. Filippakopoulos P, et al. Histone recognition and large-scale structural analysis of the human bromodomain family. *Cell.* 2012; 149:214–231. [PubMed: 22464331]
24. Ruthenburg AJ, et al. Recognition of a mononucleosomal histone modification pattern by BPTF via multivalent interactions. *Cell.* 2011; 145:692–706. [PubMed: 21596426]
25. Müller MM, Muir TW. Histones: at the crossroads of peptide and protein chemistry. *Chem. Rev.* 2015; 115:2296–2349. [PubMed: 25330018]
26. Taverna SD, Li H, Ruthenburg AJ, Allis CD, Patel DJ. How chromatin-binding modules interpret histone modifications: lessons from professional pocket pickers. *Nat. Struct. Mol. Biol.* 2007; 14:1025–1040. [PubMed: 17984965]
27. McGinty RK, Tan S. Nucleosome structure and function. *Chem. Rev.* 2015; 115:2255–2273. [PubMed: 25495456]
28. Fujiki R, et al. GlcNAcylation of histone H2B facilitates its monoubiquitination. *Nature.* 2011; 480:557–560. [PubMed: 22121020]
29. Clapier CR, Cairns BR. Regulation of ISWI involves inhibitory modules antagonized by nucleosomal epitopes. *Nature.* 2012; 492:280–284. [PubMed: 23143334]
30. Zhao S, et al. Mutational landscape of uterine and ovarian carcinosarcomas implicates histone genes in epithelial-mesenchymal transition. *Proc. Natl Acad. Sci. USA.* 2016; 113:12238–12243. [PubMed: 27791010]
31. Casadio F, et al. H3R42me2a is a histone modification with positive transcriptional effects. *Proc. Natl Acad. Sci. USA.* 2013; 110:14894–14899. [PubMed: 23980157]
32. McGinty RK, et al. Structure-activity analysis of semisynthetic nucleosomes: mechanistic insights into the stimulation of Dot1L by ubiquitylated histone H2B. *ACS Chem. Biol.* 2009; 4:958–968. [PubMed: 19799466]
33. Biron E, Chatterjee J, Kessler H. Optimized selective N-methylation of peptides on solid support. *J. Pept. Sci.* 2006; 12:213–219. [PubMed: 16189816]
34. Brown ZZ, et al. Strategy for “detoxification” of a cancer-derived histone mutant based on mapping its interaction with the methyltransferase PRC2. *J. Am. Chem. Soc.* 2014; 136:13498–13501. [PubMed: 25180930]
35. Hackeng TM, Griffin JH, Dawson PE. Protein synthesis by native chemical ligation: expanded scope by using straightforward methodology. *Proc. Natl Acad. Sci. USA.* 1999; 96:10068–10073. [PubMed: 10468563]
36. Li XQ, Kawakami T, Aimoto S. Direct preparation of peptide thioesters using an Fmoc solid-phase method. *Tetrahedr. Lett.* 1998; 39:8669–8672.
37. Mitchell SA, Pratt MR, Hruby VJ, Polt R. Solid-phase synthesis of O-linked glycopeptide analogues of enkephalin. *J. Org. Chem.* 2001; 66:2327–2342. [PubMed: 11281773]
38. Thompson RE, et al. Trifluoroethanethiol: an additive for efficient one-pot peptide ligation-desulfurization chemistry. *J. Am. Chem. Soc.* 2014; 136:8161–8164. [PubMed: 24873761]
39. Li Y, et al. Molecular coupling of histone crotonylation and active transcription by AF9 YEATS domain. *Mol. Cell.* 2016; 62:181–193. [PubMed: 27105114]
40. Xiong X, et al. Selective recognition of histone crotonylation by double PHD fingers of MOZ and DPF2. *Nat. Chem. Biol.* 2016; 12:1111–1118. [PubMed: 27775714]
41. Batjargal S, Walters CR, Petersson EJ. Inteins as traceless purification tags for unnatural amino acid proteins. *J. Am. Chem. Soc.* 2015; 137:1734–1737. [PubMed: 25625321]
42. Barak O, Lazzaro MA, Cooch NS, Picketts DJ, Shiekhattar R. A tissue-specific, naturally occurring human SNF2L variant inactivates chromatin remodeling. *J. Biol. Chem.* 2004; 279:45130–45138. [PubMed: 15310751]
43. Phelan ML, Sif S, Narlikar GJ, Kingston RE. Reconstitution of a core chromatin remodeling complex from SWI/SNF subunits. *Mol. Cell.* 1999; 3:247–253. [PubMed: 10078207]

44. Dyer PN, et al. Reconstitution of nucleosome core particles from recombinant histones and DNA. *Methods Enzymol.* 2004; 375:23–44. [PubMed: 14870657]
45. Flaus A, Richmond TJ. Positioning and stability of nucleosomes on MMTV 3′LTR sequences. *J. Mol. Biol.* 1998; 275:427–441. [PubMed: 9466921]

Author Manuscript

Author Manuscript

Author Manuscript

Author Manuscript

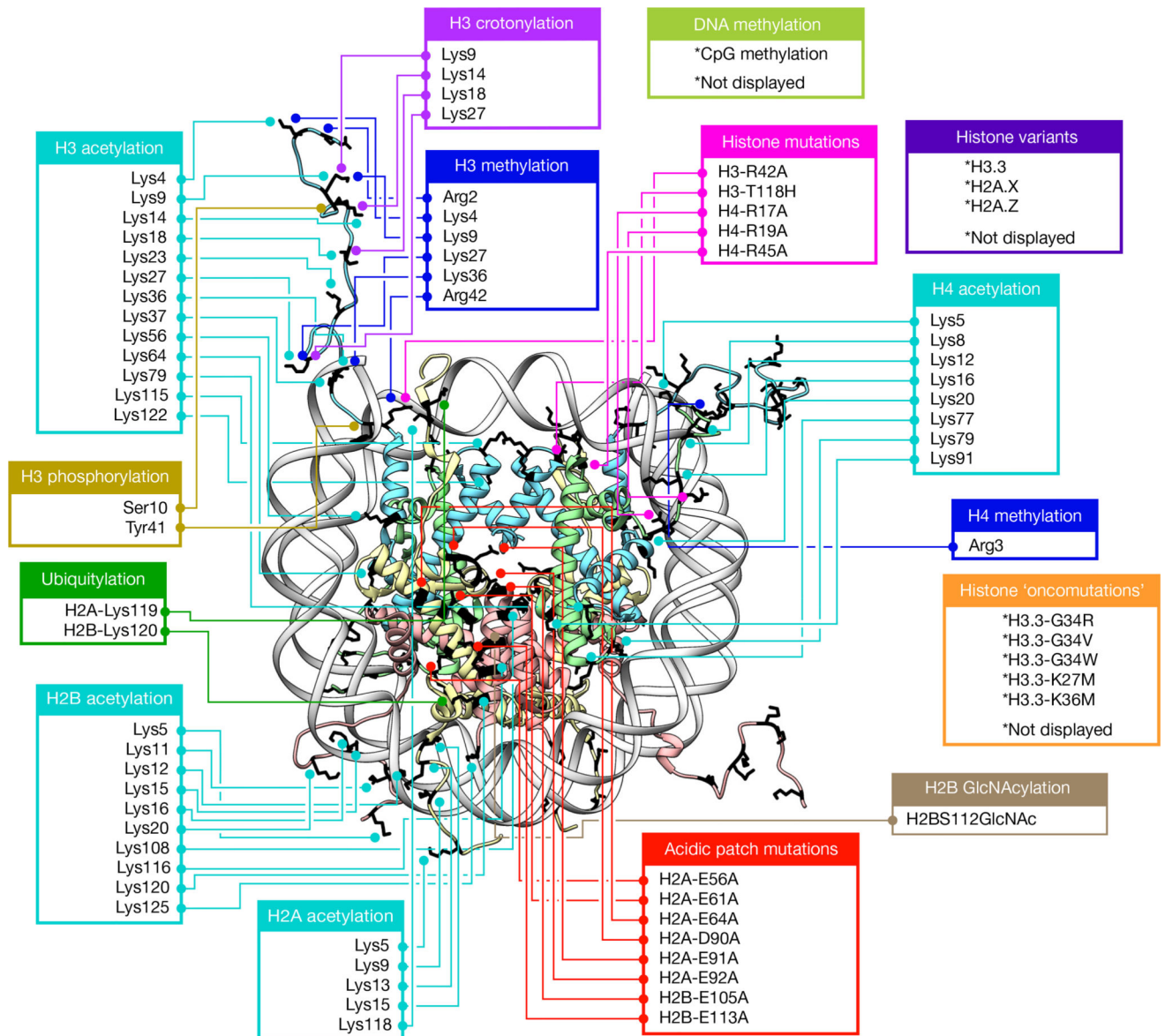


Figure 1. A diverse library of modified nucleosomes

Diagram depicting all histone modifications, mutants, and variants present in the 115-member nucleosome library used in this study. Residues modified or mutated were mapped on to the nucleosome (PDB: 1KX5) in black using UCSF Chimera. H2A (light yellow), H2B (light red), H3 (light blue) and H4 (light green) modification and mutation locations are indicated by boxes and lines. For clarity, connections are shown to only a single copy of each histone protein.

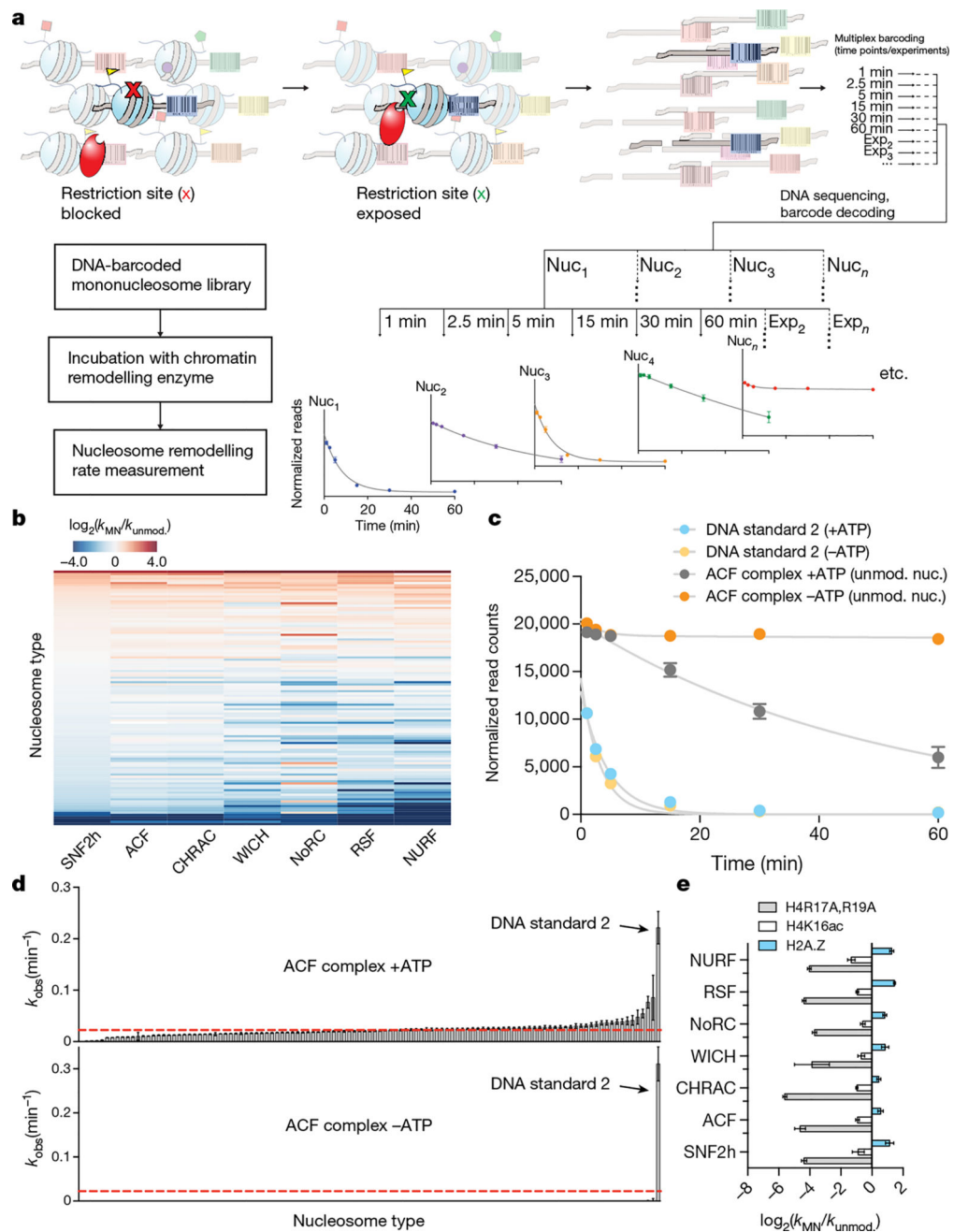


Figure 2. A high-throughput nucleosome remodelling assay for ISWI family chromatin remodellers

a, Schematic of the restriction enzyme accessibility assay used with the DNA-barcoded library. Individual remodelling rates are calculated from unique DNA sequencing reads. **b**, Heat map displaying ISWI remodelling data against the nucleosome library. Rows were sorted on the basis of values for SNF2h (low to high). k_{MN} , nucleosome remodelling rate; $k_{unmod.}$, unmodified nucleosome remodelling rate. Values were capped at -4 and 4 for display purposes. **c**, Example decay curves depicting individual rates (k_{MN}) as in **b**. **d**, Rank-ordered remodelling rates for the ACF complex (k_{MN}) against the library. Dashed red line,

k_{unmod} **e**, Relative remodelling rates as in **b** for select library members. All data are represented as the mean of experimental replicates ($n = 3$). Error bars represent s.e.m. All histones are unmodified unless otherwise specified.

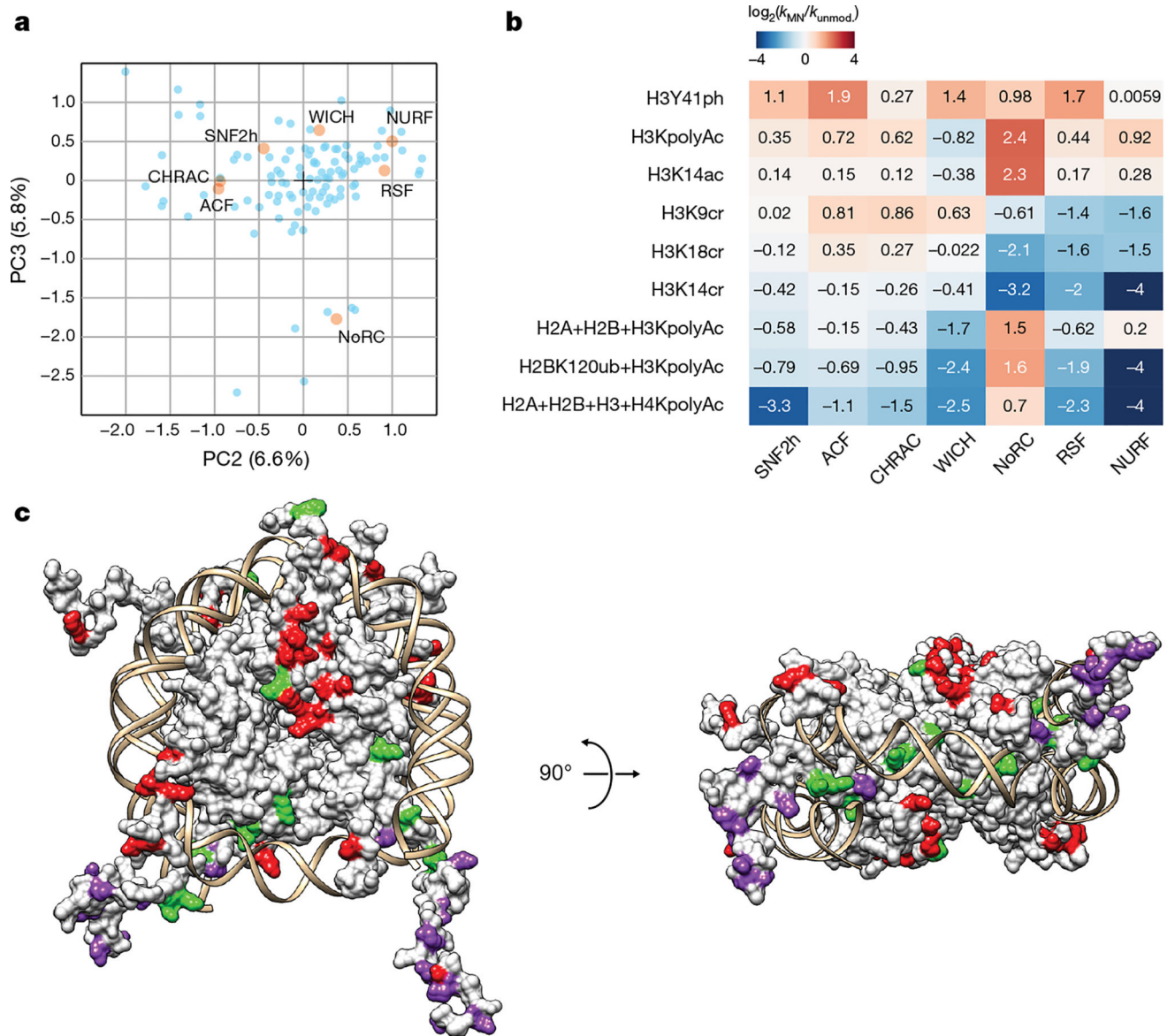


Figure 3. Specialization of ISWI remodellers for diverse nucleosome modifications

a, Principal component analysis of library remodelling data. Nucleosomes, light blue; principal component (PC) weight values for remodellers, orange. Weights are scaled by a factor of 2 for visibility. **b**, ISWI remodelling data for selected nucleosome substrates in the library. Values capped at -4 and 4 for display purposes. All histones are unmodified unless otherwise specified. **c**, Single-site modifications mapped onto the nucleosome (PDB: 1KX5) and coloured according to whether they had consistently positive (green), consistently negative (red), or variable (purple) effects on nucleosome remodelling activity across all ISWI remodellers analysed.

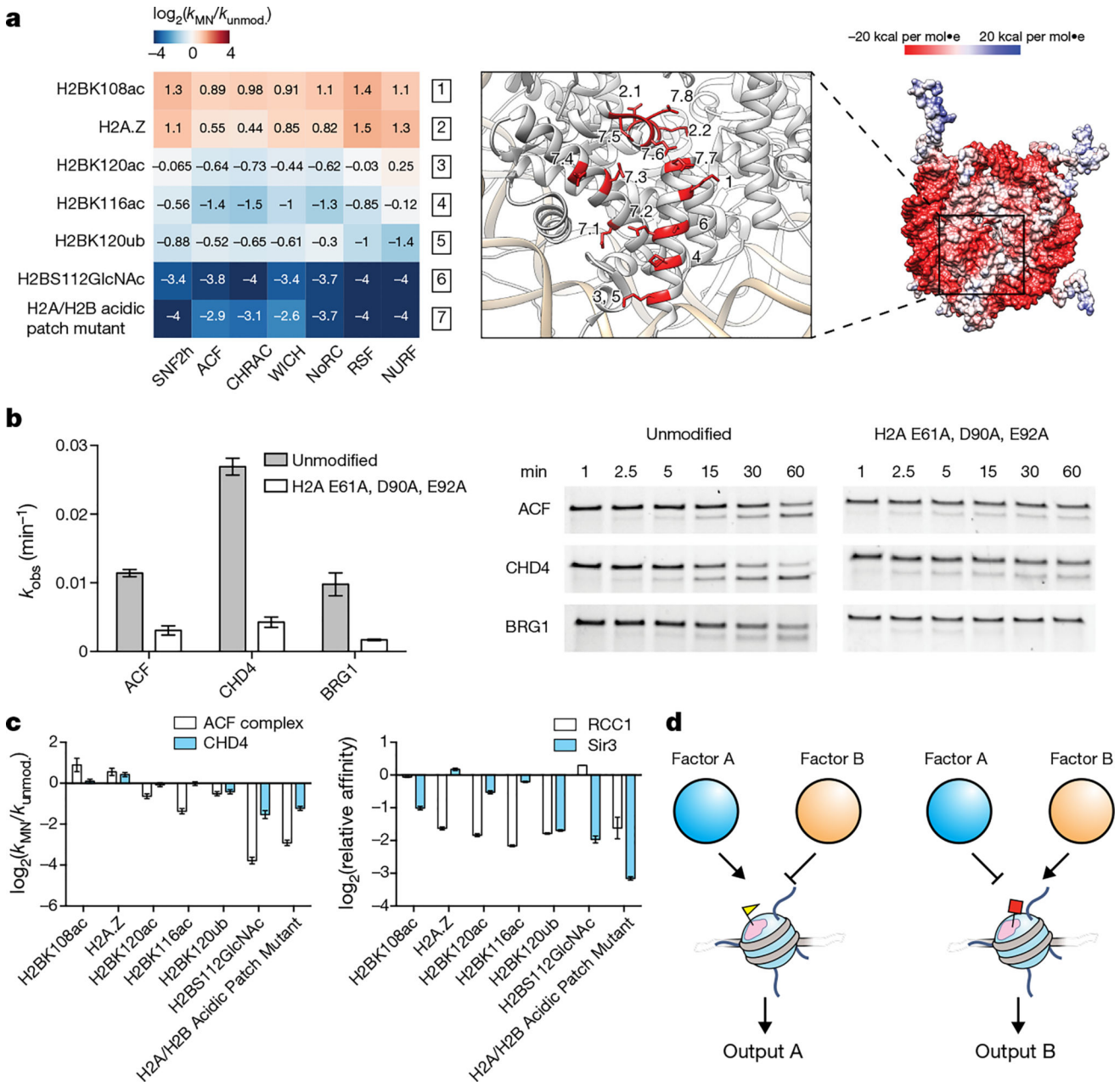


Figure 4. The nucleosome acidic patch is crucial for remodelling and regulatable by histone PTMs

a, Right, Coulombic surface rendering of the nucleosome (PDB: 1KX5). Left, effect of acidic patch modifications and mutations on ISWI remodelling activity. Mutations and PTM locations are individually numbered on the nucleosome structure (middle) with decimals indicating multiple changes per nucleosome (7.1, H2AE56A; 7.2, H2BE113A; 7.3, H2AE61A; 7.4, H2AE64A; 7.5, H2AD90A; 7.6, H2AE92A; 7.7, H2BE105A; 7.8, H2AE91A; 2.1, N94D (H2A → H2A.Z); 2.2, K95S (H2A → H2A.Z)). Values capped at -4 and 4 for display purposes. **b**, E61A, D90A, and E92A mutations in H2A reduce remodelling activity of the ACF complex, CHD4, and BRG1 as read out by a gel-based restriction enzyme accessibility assay (corresponding example replicates shown on right). **c**,

Acidic patch modifications differentially affect remodelling activity and binding of chromatin factors relative to unmodified nucleosomes. For complete datasets see Extended Data Fig. 9, Supplementary Table 3 and Supplementary Table 7. **d**, Model of how histone modifications (yellow triangle, red square) proximal to the acidic patch (pink) might differentially regulate the binding and function of chromatin factors. For **a–c** all histones are unmodified unless otherwise specified. For **b** and **c** data are represented as the mean of experimental replicates ($n = 3$). Error bars represent s.e.m. For gel source data, see Supplementary Fig. 1.

Author Manuscript

Author Manuscript

Author Manuscript

Author Manuscript